



January 2019

# Synthesis Of Biodegradable Star-Shaped Polymers Using Bio-Based Polyols Via Ring-Opening Polymerization Of B-Butyrolactone With Amido-Oxazolate Zinc Catalysts

Rawan Omar

Follow this and additional works at: <https://commons.und.edu/theses>

---

## Recommended Citation

Omar, Rawan, "Synthesis Of Biodegradable Star-Shaped Polymers Using Bio-Based Polyols Via Ring-Opening Polymerization Of B-Butyrolactone With Amido-Oxazolate Zinc Catalysts" (2019). *Theses and Dissertations*. 2479.  
<https://commons.und.edu/theses/2479>

This Thesis is brought to you for free and open access by the Theses, Dissertations, and Senior Projects at UND Scholarly Commons. It has been accepted for inclusion in Theses and Dissertations by an authorized administrator of UND Scholarly Commons. For more information, please contact [zeinebyousif@library.und.edu](mailto:zeinebyousif@library.und.edu).

SYNTHESIS OF BIODEGRADABLE STAR-SHAPED POLYMERS USING BIO-BASED  
POLYOLS VIA RING-OPENING POLYMERIZATION OF  $\beta$ -BUTYROLACTONE WITH  
AMIDO-OXAZOLINATE ZINC CATALYSTS

by

Rawan Ibrahim Omar  
Bachelor of Science, King Abdulaziz University, 2013

A Thesis

Submitted to the Graduate Faculty

of the

University of North Dakota

in partial fulfillment of the requirements

for the degree of

Master of Science

Grand Forks, North Dakota

May


2019

Copyright 2019 Rawan Omar

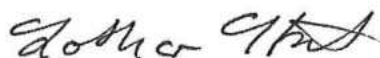
This thesis, submitted by Rawan Omar in partial fulfillment of the requirements for the Degree of Master of Science from the University of North Dakota, has been read by the Faculty Advisory Committee under whom the work has been done and is hereby approved.



Committee Chairperson – Dr. Guodong Du

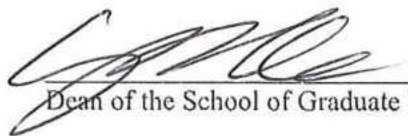


Committee Member – Dr. Harmon B. Abrahamson



Committee Member – Dr. Lothar Stahl

This thesis is being submitted by the appointed advisory committee as having met all of the requirements of the School of Graduate Studies at the University of North Dakota and is hereby approved.



Dean of the School of Graduate Studies

4/30/19

Date

## PERMISSION

Title	Synthesis of Biodegradable Star-Shaped Polymers Using Bio-Based Polyols via Ring-Opening Polymerization of $\beta$ -Butyrolactone with Amido-Oxazolate Zinc Catalysts
Department	Chemistry
Degree	Master of Science

In presenting this thesis in partial fulfillment of the requirements for a graduate degree from the University of North Dakota, I agree that the library of this University shall make it freely available for inspection. I further agree that permission for extensive copying for scholarly purposes may be granted by the professor who supervised my thesis work or, in his absence, by the Chairperson of the department or the dean of the School of Graduate Studies. It is understood that any copying or publication or other use of this thesis or part thereof for financial gain shall not be allowed without my written permission. It is also understood that due recognition shall be given to me and to the University of North Dakota in any scholarly use which may be made of any material in my thesis.

Rawan Omar

March 19, 2019

## ABBREVIATIONS

Al <sub>2</sub> O <sub>3</sub>	Aluminum Oxide
BBL	β-Butyrolactone
BINAP	Bis(diphenylphosphino)-1,1'-binaphthyl
BnOH	Benzyl Alcohol
CaH <sub>2</sub>	Calcium Hydride
C <sub>6</sub> D <sub>6</sub>	Deuterated Benzene
CDCl <sub>3</sub>	Deuterated Chloroform
CO <sub>2</sub>	Carbon Dioxide
1,4-CHD	1,4-Cyclohexanediol
DCM	Dichloromethane
DSC	Differential Scanning Calorimetry
Đ	Polydispersity Index
EtOH	Ethyl Alcohol
GPC	Gel Permeation Chromatography
HSSP	Hydroxylated sucrose Soyate Polyol
<i>M<sub>n</sub></i>	Number-Average Molecular Weight
MSSP	Methoxylated Sucrose Soyate Polyol
MW	Molecular Weight
NMR	Nuclear Magnetic Resonance Spectroscopy

$\text{Pd}(\text{OAc})_2$	Palladium Acetate
PE	Pentaerythritol
PHA	Polyhydroxyalkanoates
PHB	Poly( $\beta$ -hydroxybutyrate)
$P_r$	Probability of <i>racemic</i> diads
ROP	Ring-Opening Polymerization
ROCOP	Ring-Opening Copolymerization
<i>t</i> -BuONa	Sodium <i>t</i> -Butoxide
TGA	Thermogravimetric Analysis
THF	Tetrahydrofuran
$t$	Time
$T_g$	Glass Transition Temperature
$T_m$	Melting Temperature
$\text{Zn}[\text{N}(\text{SiMe}_3)_2]_2$	Zinc Bis[bis(trimethylsilyl)amide]

## TABLE OF CONTENTS

LIST OF TABLES.....	ix
LIST OF FIGURES .....	x
LIST OF SCHEMES .....	x
ACKNOWLEDGMENTS .....	xiii
ABSTRACT.....	xiv
CHAPTER 1 .....	1
1.1 Introduction .....	1
1.2 Poly( $\beta$ -Hydroxybutyrate) .....	1
1.3 Star-Shaped Poly( $\beta$ -Hydroxybutyrate).....	5
REFERENCES .....	7
CHAPTER 2 .....	12
2.1 Introduction .....	12
2.2 Experiment Section.....	14
2.2.1 Materials and Methods .....	14
2.2.2 Synthesis of the Zinc Complex .....	15
2.2.3 General Procedure for ROP of BBL .....	15



2.3	Results and Discussion .....	18
2.3.1	ROP of BBL with Glycerin.....	18
2.3.2	ROP of BBL with Pentaerythritol .....	22
2.3.3	ROP of BBL with Polyols.....	28
2.4	Thermal Properties .....	33
2.5	Thermogravimetric Analysis .....	38
	Conclusions .....	39
	REFERENCES .....	40

## LIST OF TABLES

<b>Table 1.</b> ROP of <i>rac</i> - $\beta$ -butyrolactone using catalyst <b>1</b> with glycerin. <sup>a</sup> .....	19
<b>Table 2.</b> ROP of <i>rac</i> - $\beta$ -butyrolactone using catalyst <b>1</b> with pentaerythritol. <sup>a</sup> .....	23
<b>Table 3.</b> ROP of <i>rac</i> - $\beta$ -butyrolactone using catalyst <b>1</b> with MSSP and HSSP. <sup>a</sup> .....	30
<b>Table 4.</b> Thermal properties of star-shaped PHBs. <sup>a,b</sup> .....	34
<b>Table 5.</b> Thermal properties of PHBs with glycerin with different arm lengths. <sup>a,b</sup> .....	37
<b>Table 6.</b> Thermal properties of PHBs with PE with different arm lengths. <sup>a,b</sup> .....	37
<b>Table 7.</b> Thermal properties of PHBs with MSSP with different arm lengths. <sup>a,b</sup> .....	37

## LIST OF FIGURES

<b>Fig. 1.</b> Synthetic routes of PHBs. ....	4
<b>Fig. 2.</b> The available microstructures of PHB's main-chain. ....	4
<b>Fig. 3.</b> The synthetic routes for star-shaped polymers.....	7
<b>Figure 1.</b> $^1\text{H}$ -NMR spectrum of the PHB with glycerin as a central core.....	21
<b>Figure 2.</b> $^{13}\text{C}$ -NMR spectrum of the PHB with glycerin as a central core.....	21
<b>Figure 3.</b> $^1\text{H}$ - $^{13}\text{C}$ COSY NMR spectrum of the PHB with glycerin as a central core.....	22
<b>Figure 4.</b> Conversion as a function of reaction time for the polymerization of BBL with PE in toluene, $T = 100\text{ }^\circ\text{C}$ . Polymerization was initiated with catalyst <b>1</b> . [catalyst <b>1</b> ]:[PE]:[BBL] = 4:1:800. ....	24
<b>Figure 5.</b> Plot of BBL monomer conversion expressed as $-\ln([M]/[M]_0)$ versus reaction time for polymerization initiated with PE initiator, $[M]/[I] = 400$ , as monitored by $^1\text{H}$ -NMR spectroscopy in $\text{CDCl}_3$ .....	25
<b>Figure 6.</b> $^1\text{H}$ -NMR spectrum of the PHB with pentaerythritol as a central core. ....	26
<b>Figure 7.</b> $^{13}\text{C}$ -NMR spectrum of the PHB with pentaerythritol as a central core.....	27
<b>Figure 8.</b> $^1\text{H}$ - $^{13}\text{C}$ COSYNMR spectrum of the PHB with pentaerythritol as a central core.....	28
<b>Figure 9.</b> Molecular structure of the MSSP and HSSP core initiators.....	29

<b>Figure 10.</b> $^1\text{H}$ -NMR spectrum of the PHB with MSSP as a central core in $\text{CDCl}_3$ : MSSP core (bottom), and $[\text{M}]/[\text{I}] = 4800$ (Table 3, entry 4) (top). .....	32
<b>Figure 11.</b> $^1\text{H}$ -NMR spectrum of the PHB with HSSP as a central core in $\text{CDCl}_3$ : HSSP core (bottom), and $[\text{M}]/[\text{I}] = 2400$ (Table 3, entry 6) (top). .....	33
<b>Figure 12.</b> DSC analysis of star-shaped PHBs.....	35
<b>Figure 13.</b> DSC analysis of star-shaped PHBs with glycerin with different arm lengths.....	35
<b>Figure 14.</b> DSC analysis of star-shaped PHBs with PE with different arm lengths. ....	36
<b>Figure 15.</b> DSC analysis of star-shaped PHBs with MSSP with different arm lengths.....	36
<b>Figure 16.</b> TGA analysis of star-shaped PHBs. ....	38

## LIST OF SCHEMES

<b>Scheme 1.</b> Chiral Amido-Oxazolate Zinc Complex (Catalyst 1).....	16
<b>Scheme 2.</b> Synthetic route of various-armed star-shaped PHBs. ....	17
<b>Scheme 3.</b> Synthesis of 3-armed star-shaped polymers. ....	19
<b>Scheme 4.</b> Synthesis of 4-armed star-shaped polymers. ....	23
<b>Scheme 5.</b> Synthesis of star-shaped and highly branched PHBs the presence of MSSP and HSSP. .....	30

## ACKNOWLEDGMENTS

I would like to express my deepest appreciation to my research advisor, professor Guodong Du, he has been continuously supportive and encouraging my research. I would like to thank him for allowing me to grow as a graduate research scientist in chemistry. He has been a tremendous supervisor for me.

I would like to thank the faculty, staff, graduate students, and to all those who provided me the possibility to complete my inspirations in the department of chemistry at the University of North Dakota. In particular, I want to thank my thesis committee members, Dr. Harmon Abrahamson and Dr. Lothar Stahl for affording me support during these two years of my graduate study.

I am forever indebted to my family for everything they have done for me, especially my husband, Yasser, for his continuous support throughout my time in graduate school. I could not have done it without him. I am especially grateful to my beautiful children, Rami and Rose who are the pride and joy of my life, and I appreciate all your patience and support through my study. I also owe a special thanks to my family, my mom and dad, who have supported me over my life and encouraged me to pursue this degree.

A very special word of thanks goes for my friend, Maram. She has always been a major source of support when things would get a bit discouraging throughout my graduate study. I am also very grateful for all graduate students in our department, with whom I have shared beautiful moments in my life. Thank you, guys, for always being there for me.

## ABSTRACT

A new series of star-shaped and highly branched poly( $\beta$ -hydroxybutyrates) (PHBs) with a distinct structure was synthesized by ring-opening polymerization (ROP) of  $\beta$ -butyrolactone (BBL) with amido-oxazolate zinc catalysts. The ROP of BBL using multifunctional hydroxyl-terminated initiators is an efficient methodology that allowed the preparation of PHBs with not only well-controlled molecular weights ( $M_n$ ) and narrow dispersity ( $\mathcal{D}$ ), but also well-defined end-functional groups. Furthermore, the modifications of star-shaped and highly branched PHBs resulted in various architectures with tailored properties for many applications particularly for the biomedical field. Star-shaped structure is constructed via a core-first approach, in which the multifunctional alcohols will serve as the initiator for ROP. Specifically, three-, four-, and multi-armed star polymers were obtained and thoroughly characterized by various techniques such as nuclear magnetic resonance (NMR) spectroscopy, gel permeation chromatography (GPC), and their thermal and mechanical properties were investigated by thermogravimetric analysis (TGA) and differential scanning calorimetry (DSC). These properties were compared with the linear PHBs since it is expected that branched architectures may have different features. Moreover, the impact of the arm numbers and the arm lengths was studied on thermal properties of the obtained star-shaped PHBs, which strongly depended upon their arm numbers and arm lengths.

## CHAPTER 1

### 1.1 Introduction

Despite the significant development of polymer science, the accumulation of plastic materials and the problems related to their chemical and biological resistance have become a major concern for many researchers during the last decades.<sup>1</sup> Most of these materials are derived from petrochemical resources and could potentially have serious adverse effects to the environment due to their resistance to degradation related to the strong carbon-carbon bond in the polymer structure.<sup>2</sup> Therefore, biodegradable polymers that derived from renewable resources have been proposed as an alternative solution.<sup>1</sup> Significant efforts have been made for the development of environmentally friendly plastics using a variety of biomass and biodegradable components incorporated into polymeric structures. In which, biodegradable polymers can be eventually converted to water, carbon dioxide (CO<sub>2</sub>) and biomass in the environment by bacterial activity.<sup>3</sup> A variety of biodegradable polymers have been recently synthesized such as aliphatic polyesters, in particular, poly(lactic acid) (PLA), poly(glycolic acid) (PGA), poly( $\epsilon$ -caprolactone) (PCL), and poly(hydroxyalkanoates) (PHA). These polymers have received much attention due to their renewability, biocompatibility, and biodegradability properties and are highly desirable in industrial, medical, agriculture, and food packaging applications.<sup>4</sup> Among these polyester is poly( $\beta$ -hydroxybutyrate) (PHB), which belongs to PHA, that is one of the most promising biodegradable materials for medical applications.<sup>2</sup> To date, considerable attempts have been made to improve the properties of PHBs with a variety of architectures including linear, cross-linked, grafted, star-shaped, and hyperbranched structures for their potential applications.



## 1.2 Poly( $\beta$ -Hydroxybutyrate)

Poly( $\beta$ -hydroxybutyrate) (PHB) is a thermoplastic polymer, which can be naturally produced by a wide range of microorganisms (bacteria). PHB was first isolated by a French microbiologist in 1925 from *Bacillus megaterium*,<sup>5</sup> where the microorganisms use PHB as an energy storage facility.<sup>5</sup> Microbial PHBs have a semicrystalline isotactic structure that has exclusively the (R)-configuration, with high melting temperature ( $T_m$ ) and a glass transition temperature ( $T_g$ ) of 5 °C. In contrast, PHB resulting from chemical synthesis produced an amorphous atactic structure.<sup>6</sup> Indeed, its high melting point and low thermal decomposition temperature (190-220°C) limit its application in the industry.<sup>7</sup>

The most common methods for the synthesis of PHBs include the polycondensation and the ring-opening polymerization (ROP) of  $\beta$ -butyrolactone (BBL) as shown in Fig. 1. The polycondensation is a reversible reaction, and it is difficult to obtain high molecular weight materials due to the problem of effectively removing water formed during the reaction.<sup>8</sup> Recent improvements in the synthesis of PHBs through polycondensation method have been implemented such as chain-extension reaction and azeotropic dehydration condensation.<sup>9-12</sup> To date, ROP of BBL with metal-based catalytic systems is the convenient, well-controlled and effective synthetic methodology for obtaining high molecular weight ( $M_n$ ) PHBs, and it allows for control of the polymer chain stereochemistry.<sup>13</sup> Therefore, investigations have been directed to the synthesis of metal complexes with various ligands, including porphyrin, phenoxide, and salen-types, and their activities of promoting the transformation.<sup>14</sup> For instance, Carpentier and co-workers have reported highly active scandium and yttrium complexes supported by tetradentate diamino- or alkoxy-amino-bis(phenolate) ligands for the stereoselective ring-opening polymerization of *rac*-BBL, whereas a yttrium complex showed remarkable performance at 20 °C to afford a significantly

syndiotactic PHB, with  $P_r$  in the range 0.81–0.88.<sup>15</sup> Cui and co-workers have synthesized rare-earth metal amide complexes stabilized by salan-type ligands, and these complexes catalyzed the ROP of *rac*-BBL to give PHBs with high molecular weights. They discovered that the polymerization activity was related to the metallic covalent radius, where the larger metal center resulted in a higher observed polymerization activity. Moreover, the tacticity was significantly affected by the substituents on the bridging N atoms on the ligand frameworks.<sup>16</sup> In this regard, metal complexes with adjustable ligands play a fundamental role over molecular weight, dispersity ( $\bar{D}$ ), and the production of stereoregularity of the polymer chain (tacticity). The presence of a stereogenic center (a chiral center) in the PHB repeating unit leads to the formation of different microstructures, in which the steric order or tacticity can be defined as the relative stereochemistry of the adjacent stereogenic centers along the polymer chain within a macromolecule.<sup>13</sup> Fig. 2 shows the available microstructures of PHB's main-chain (atactic, syndiotactic, and isotactic). Atactic PHB can be obtained when all the chiral centers are randomly arranged throughout the polymer chain. If all chiral centers have the same configuration on the polymer chain, it produces isotactic PHB, and if the chiral centers alternate from one side to another along the polymer chain, the obtained PHB will have syndiotactic microstructure.

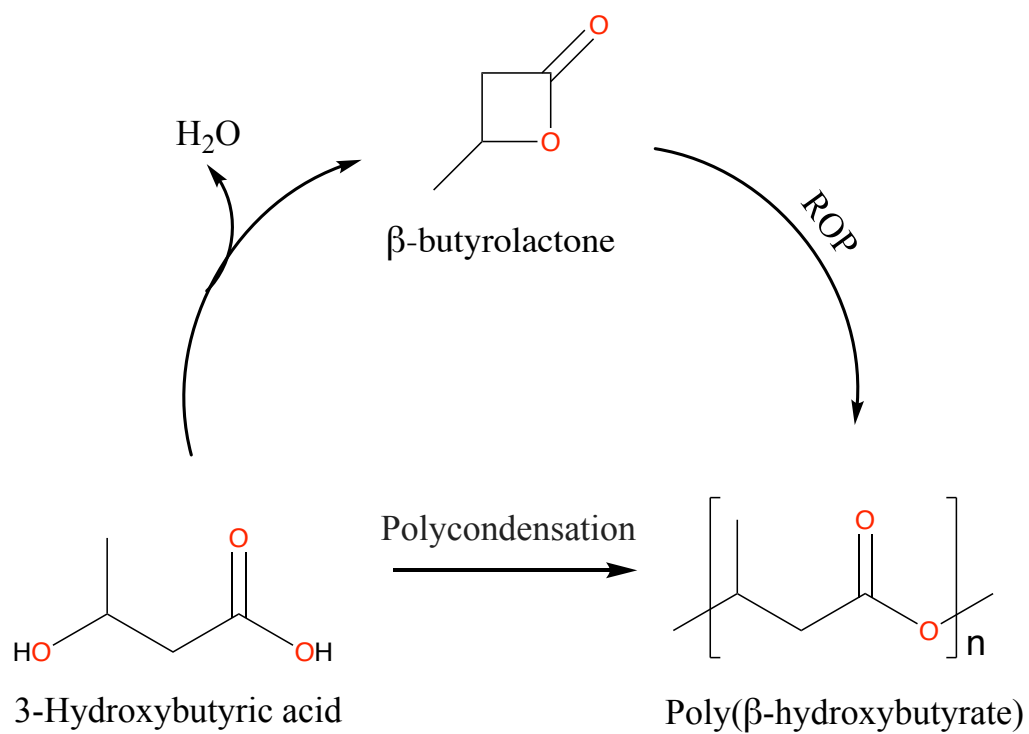


**Fig. 1.** Synthetic routes of PHBs.

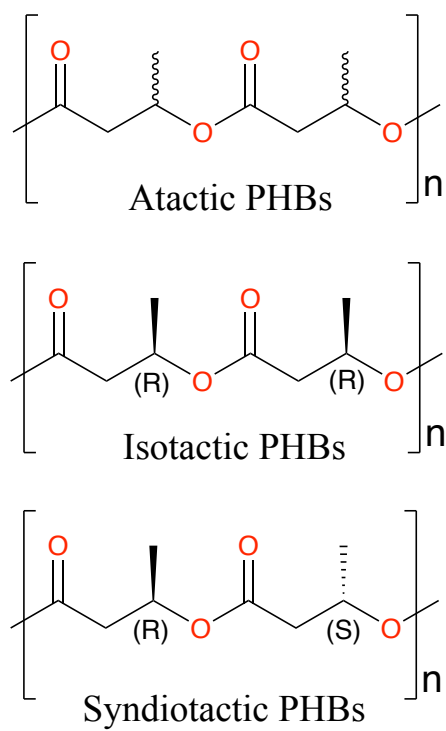


**Fig. 2.** The available microstructures of PHB's main-chain.

### 1.3 Star-Shaped Poly( $\beta$ -Hydroxybutyrate)

Star-shaped and highly branched poly( $\beta$ -hydroxybutyrate)s (PHBs) materials with well-defined architectures have recently gained much interest due to their unique structure and topological properties that set them apart from linear PHBs.<sup>12</sup> Star-shaped polymers are branched, consisting of a branched core and several linear chains in which the linear arms radiate from the core.<sup>17</sup> Homogenous star polymers are polymers in which the arms are all equivalent in length and structure, whereas heterogeneous star-shaped polymers contain variable lengths and structures. Star-shaped polymers have low melt-viscosity, smaller hydrodynamic radii, high-molecular weight, and higher functional group concentrations.<sup>18</sup> One of the most attractive applications of PHBs is in the biomedical field, especially as drug delivery systems.<sup>19</sup> However, there are only a few reports on the preparation of star-shaped PHBs, and the detailed studies are rare due to the difficulties inherent in ring-opening polymerization of BBL.

The efficient synthetic routes for star-shaped polymers are the “core-first”, “arm-first”, and “grafting-onto” approaches (Fig. 3).<sup>20</sup> In the core-first approach, a multifunctional initiator as the core initiates the polymerization to form multi-arm star polymers, radiating out from the core. In order to obtain well-defined macromolecules with the same arm number and arm length, the initiating sites must all have an equivalent degree of reactivity, and the rate of initiation must be greater than that of propagation. The only limitation of this approach is that the polymers usually tend to have low arm numbers, whereas a pure star polymer with a high yield can be obtained. In the arm-first approach, the star polymers are formed by crosslinking linear polymers through a polymerization or coupling reaction. In the grafting-onto approach, the preparation of the core and the arms before forming the final star architecture allows the highest level of structural control. Among them, the “core-first” approach is more readily available, and therefore has attracted a

great deal of interest for producing well-defined multi-armed polymeric architectures with a range of predefined numbers in the multi-functional initiators.<sup>21</sup> Therefore, star-shaped PHBs can be synthesized through ROP of BBL, following a core-first strategy, in the presence of metal-based catalysts using multifunctional hydroxyl-terminated initiators, affording good control over molecular weight, dispersity ( $\bar{M}_w/\bar{M}_n$ ), stereoselectivity, and well-defined chain end functionality.<sup>22</sup> Furthermore, several synthetic strategies were developed for the preparation of star-shaped PHBs.

Using multi-functional alcohols as the branching center will lead to a wide variety of molecular architectures. Different multi-functional initiators have been employed in star-shaped structures, including tris(hydroxymethyl)benzene, erythritol, and dipentaerythritol. Whereas, the number of the arms containing the polymer chains can be defined by the number of functional groups present in the initiator. The monomer ratio to the initiator plays an essential role to determine the number of the arm, which increases by increasing this ratio. Other parameters influence the number of branches involving the position of the hydroxyl group in the core, the concentration and the molecular weight of the living polymer chain, and the temperature and the time of the reaction.<sup>23</sup>

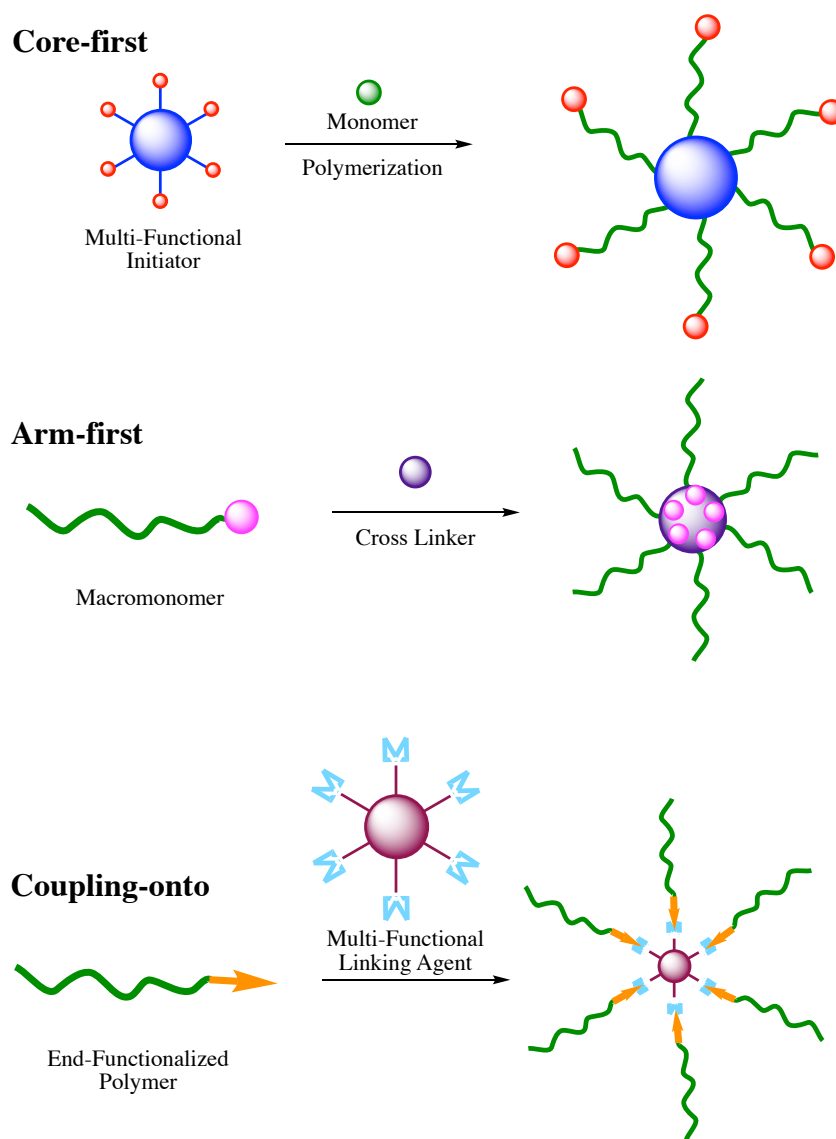


**Fig. 3.** The synthetic routes for star-shaped polymers.

Developments in the synthesis and characterization techniques have allowed the preparation of advanced architectures with unique properties inherited from the functional moieties. Our aims will concentrate on the synthesis and the characterization of star-shaped poly( $\beta$ -hydroxybutyrates) (PHBs) with tailored functionalities. Furthermore, the effect of arm numbers

and arm lengths on thermochemical properties such as glass transition temperature ( $T_g$ ) and thermal degradation of star-shaped PHBs will be discussed.

## REFERENCES

1. Rydz, J.; Sikorska, W.; Kyulavska, M.; Christova, D. Polyester-Based (Bio)degradable Polymers as Environmentally Friendly Materials for Sustainable Development. *Int. J. Mol. Sci.* **2015**, *16*, 564–596.
2. Getachew, A.; Woldesenbet, F. Production of Biodegradable Plastic by Polyhydroxybutyrate (PHB) Accumulating Bacteria Using Low Cost Agricultural Waste Material. *Getachew Woldesenbet BMC Res. Notes.* **2016**, *9*, 509–518.
3. Song, J. H.; Murphy, R. J.; Narayan, R.; Davies, G. B. H. Biodegradable and Compostable Alternatives to Conventional Plastics. *Phil. Trans. R. Soc. B. Biol. Sci.* **2009**, *364*, 2127–2139.
4. Philip, S.; Keshavarz, T.; Roy, I. Polyhydroxyalkanoates: Biodegradable Polymers with a Range of Applications. *J. Chem. Technol. Biotechnol.* **2007**, *82*, 233–247.
5. Norris, K. P.; Greenstreet, J. E. S. On the Infrared Absorption Spectrum of *Bacillus Megaterium*. *J. Gen. Microbiol.* **1958**, *19*, 566–580.
6. Zintl, M.; Molnar, F.; Urban, T.; Bernhart, V.; Pflügl, P. P.; Rieger, B. Variably Isotactic Poly(hydroxybutyrate) from Racemic  $\beta$ -Butyrolactone: Microstructure Control by Achiral Chromium(III) Salophen Complexes. *Angew. Chem. Int. Ed.* **2008**, *47*, 3458–3460.

7. Jiang, N.; Abe, H. Effect of Atactic Poly(3-hydroxybutyrate) Block on the Crystallization and Degradation Behavior of 6-arm Poly(L-lactide)-b-Atactic Poly(3-hydroxybutyrate). *Polym. Degradation Stability* **2015**, *114*, 8–15.
8. Kobayashi, S. Enzymatic Ring-Opening Polymerization and Polycondensation for the Green Synthesis of Polyesters. *Polym. Adv. Technol.* **2015**, *26*, 677–686.
9. Macdonald, E. K.; Shaver, M. P. Understanding the Phosphoric Acid Catalyzed Ring Opening Polymerisation of  $\beta$ -Butyrolactone and Other Cyclic Esters. *Europ. Polym. J.* **2017**, *95*, 702–710.
10. Luciano, E.; Buonerba, A.; Grassi, A.; Milione, S.; Capacchione, C. Thioetherphenolate Group 4 Metal Complexes in the Ring-Opening Polymerization of *rac*- $\beta$ -Butyrolactone. *Polym. Chem.* **2016**, *54*, 3132–3139.
11. Ajellal, N.; Bouyahyi, M.; Amgoune, A.; Thomas, C. M.; Bondon, A.; Pillin, I.; Grohens, Y.; Carpentier, J. F. Syndiotactic-Enriched Poly(3-hydroxybutyrate)s via Stereoselective Ring-Opening Polymerization of Racemic  $\beta$ -Butyrolactone with Discrete Yttrium Catalysts. *Macromolecules.* **2009**, *42*, 987–993.
12. Don, T. M.; Liao, K. H. Studies on the Alcoholysis of Poly(3-Hydroxybutyrate) and the Synthesis of PHB-b-PLA Block Copolymer for the Preparation of PLA/PHB-b-PLA Blends. *J. Polym. Res.* **2018**, *25*, 38–48.
13. Thomas, C. M. Stereocontrolled Ring-Opening Polymerization of Cyclic Esters: Synthesis of New Polyester Microstructures. *Chem. Soc. Rev.* **2010**, *39*, 165–173.
14. Duan, R.; Qu, Z.; Pang, X.; Zhang, Y.; Sun, Z.; Zhang, H.; Bian, X.; Chen, X. Ring-Opening Polymerization of Lactide Catalyzed by Bimetallic Salen-Type Titanium Complexes. *Chin. J. Chem.* **2017**, *35*, 640–644.



15. Chapurina, Y.; Klitzke, J.; Jr, C. O. L.; Awada, M.; Dorcet, V.; Kirillov, E.; Carpentier, J. F. Scandium Versus Yttrium {amino-alkoxy-bis- (phenolate)} Complexes for The Stereoselective Ring-Opening Polymerization of Racemic Lactide and  $\beta$ -Butyrolactone. *Dalton Trans.* **2014**, *43*, 14322–14333.
16. Zhuo, Z.; Zhang, C.; Luo, Y.; Wang, Y.; Yao, Y.; Yuan, D., Cui, D. Stereo-Selectivity Switchable ROP of *rac*- $\beta$ -Butyrolactone Initiated by Salan-Ligated Rare-Earth Metal Amide Complexes: The Key Role of The Substituents on Ligand Frameworks. *Chem. Commun.* **2018**, *54*, 11998–12001.
17. Dirlam, P. T.; Goldfeld, D. J.; Dykes, D. C.; Hillmyer, M. A. Polylactide Foams with Tunable Mechanical Properties and Wettability using a Star Polymer Architecture and a Mixture of Surfactants. *ACS Sustainable Chem. Eng.* **2019**, *7*, 1698–1706.
18. Lele, B.S.; Leroux, J.C. Synthesis of Novel Amphiphilic Star-Shaped Poly(1-caprolactone)-Block- Poly(N-(2-hydroxypropyl)methacrylamide) by Combination of Ring-Opening and Chain Transfer Polymerization. *Polymer* **2002**, *43*, 5595–5606.
19. Yu, I.; Ebrahimi, T.; Hatzikiriakos, S. G.; Mehrkhodavandi, P. Star-Shaped PHB–PLA Block Copolymers: Immortal Polymerization with Dinuclear Indium Catalysts. *Dalton Trans.* **2015**, *44*, 14248–14254.
20. Ren, J. M.; McKenzie, T. G.; Fu, Q.; Wong, E. H. H.; Xu, J.; An, Z.; Shanmugam, S.; Davis, T. P.; Boyer, C.; Qiao, G. G. Star Polymers. *Chem. Rev.* **2016**, *116*, 6743–6836.
21. Michalski, A.; Brzezinski, M.; Lapienis, G.; Biela, T. Star-Shaped and Branched Polylactides: Synthesis, Characterization, and Properties. *Prog. Polym. Sci.* **2019**, *89*, 159–212.

22. Teng, L.; Xu, X.; Nie, W.; Zhou, Y.; Song, L.; Chen, P. Synthesis and Degradability of a Star-Shaped Polylactide Based on *L*-Lactide and Xylitol. *J. Polym. Res.* **2015**, *22*, 83–45.
23. Lapienis, G. Star-Shaped Polymers Having PEO Arms. *Prog. Polym. Sci.* **2009**, *34*, 852–892.

## CHAPTER 2

### 2.1 Introduction

Aliphatic polyesters such as poly(hydroxyalkanoates) (PHAs) have recently received much interest as an environmentally friendly biomaterial, and they have been widely used in a variety of applications, ranging from the packaging industry to medicine.<sup>1,2</sup> Particularly, poly( $\beta$ -hydroxybutyrate)s (PHBs) have emerged as an important class of materials possessing enhanced biodegradability, biocompatibility, renewability, thermal stability, and mechanical properties. They can be used as alternative materials for many applications instead of petroleum-based plastics.<sup>3</sup> PHBs can be naturally produced by microorganisms, which give a highly isotactic and crystalline structure that has a high melting temperature ( $T_m$ ) and a relatively low thermostability.<sup>4,5</sup> Commonly, the most convenient method used for the synthesis of PHBs is the ring-opening polymerization (ROP) of  $\beta$ -butyrolactone (BBL) with metal catalysts, which have the advantage of producing polymers with well-controlled molecular weight ( $M_n$ ) and narrow dispersity ( $\mathcal{D}$ ).<sup>6</sup> Zn complexes bearing a various set of ancillary ligands displayed high catalytic activity for ROP of cyclic esters. Despite the intensive efforts in catalyst development, detailed studies of linear or star-shaped PHBs generated through ROP of BBL are rare.<sup>7,8</sup> In recent years, an increased attention has been particularly attracted to the synthesis of star-shaped PHB due to their unique structure and topological properties that are otherwise not accessible in the case of linear polymers.<sup>9</sup> The introduction of functional alcohols as initiators or chain transfer agents into polymeric structures offers advanced architectures with unique properties inherited from the functional moieties.<sup>10</sup> The efficient synthetic routes for star-shaped polymers are the “core-first”, “arm-first”, and “grafting-onto” approaches.<sup>11</sup> Among them, the “core-first” has attracted a great deal of interest, and therefore has been extensively used for producing well-defined multi-armed

polymeric architectures with a range of predefined numbers in the multi-functional initiators.<sup>12–14</sup> Because of their peculiar morphologies and the higher functional group concentrations, star-shaped PHBs may have enhanced properties such as smaller hydrodynamic radii, lower viscosities, and thermal properties for biomedical and drug delivery applications.<sup>15–17</sup> Interestingly, Hillmyer and co-workers reported that a multi-arm star architecture of poly(lactide) (PLA) could have greater impact on preparing lower density foams with CO<sub>2</sub> than the linear analogue, enabling further reduction in foam densities and imparting persistent wettability.<sup>18</sup>

Previously, we had reported that zinc complexes bearing a chiral amido-oxazolate framework are efficient catalysts for the ROP of lactide<sup>19</sup> as well as ring-opening copolymerization (ROCOP) of epoxide with CO<sub>2</sub><sup>20,21</sup> or cyclic anhydrides.<sup>22</sup> They are also active for the controlled ROP of BBL in the presence of mono- and bifunctional alcohols such as ethyl alcohol (EtOH), benzyl alcohol (BnOH), and 1,4-cyclohexanediol (1,4-CHD), resulting in the formation of linear PHBs with well-defined end groups. Cyclic PHBs with high molecular weight (up to 197 kg/mol) were produced in the absence of an alcohol.<sup>23</sup>

In this study, we report a series of star-shaped PHBs with distinctly different initiator core structures containing functional end groups. Biobased alcohols such as glycerin and pentaerythritol (PE) were used to perform the three- and four- arms star-shaped PHBs, and the multifunctional alcohols including methoxylated sucrose soyate polyol (MSSP) and hydroxylated sucrose soyate polyol (HSSP) were employed to produce the star-shaped PHBs. The obtained polymers were thoroughly characterized and investigated for their thermal and mechanical properties by various techniques. The impact of the number and the length of the arms were studied and compared with the linear PHBs since it is expected that branched architectures may have different features. To the

best of our knowledge, experimental analyses on syntheses and thermochemical properties have not been comprehensively extended to the ROP of BBL as a monomer.

## 2.2 Experiment Section

### 2.2.1 Materials and Methods

All reactions involving air- and/or moisture-sensitive compounds were performed under a dry nitrogen atmosphere using standard Schlenk line and glovebox techniques. Deuterated solvents were purchased from Cambridge Isotope Laboratories. THF was purchased from Fisher Scientific and used as received. Toluene was distilled under nitrogen from Na/benzophenone.  $\text{CDCl}_3$  and  $\text{C}_6\text{D}_6$  were distilled over  $\text{CaH}_2$  and degassed prior to use.  $\beta$ -Butyrolactone was distilled over  $\text{CaH}_2$  following three freeze-pump-thaw cycles. Glycerin was dried over molecular sieves (4 Å) prior to use. Pentaerythritol was dried under vacuum overnight. Methoxylated sucrose soyate polyol (MSSP) and hydroxylated sucrose soyate polyol (HSSP) were prepared according to the literature<sup>24</sup> and diluted in dried toluene and stored with 4Å molecular sieves. The zinc catalyst was synthesized according to literature methods.<sup>25</sup>

NMR spectra (1D and 2D) were recorded on a Bruker AVANCE 500 NMR spectrometer and referenced to the residual peaks in  $\text{CDCl}_3$ . Gel permeation chromatography (GPC) analysis was performed on a Varian Prostar instrument equipped, with PLgel 5  $\mu\text{m}$  Mixed-D column, a Prostar 355 RI detector, and with THF as eluent at a flow rate of 1 mL/min (20 °C). Polystyrene standards were used for calibration. Thermal gravimetric analysis (TGA) of PHBs was performed on an SDT Q 600 instrument at a flow rate of 100 mL/min of  $\text{N}_2$  (furnace purge gas). The samples in Aluminum oxide ( $\text{Al}_2\text{O}_3$ ) cups were heated from 30 to 600 °C with a ramp rate of 20 °C/min. Advantage software was used to analyze the TGA data. The differential scanning calorimetry (DSC) thermograms were collected on a PerkinElmer Jade differential scanning calorimeter, and

the instrument was calibrated using zinc and indium standards using 20.0 °C/min heating rate from -20 °C to 160 °C with 20 mL/min nitrogen flow. DSC data were analyzed using Pyris V9.0.2 software.

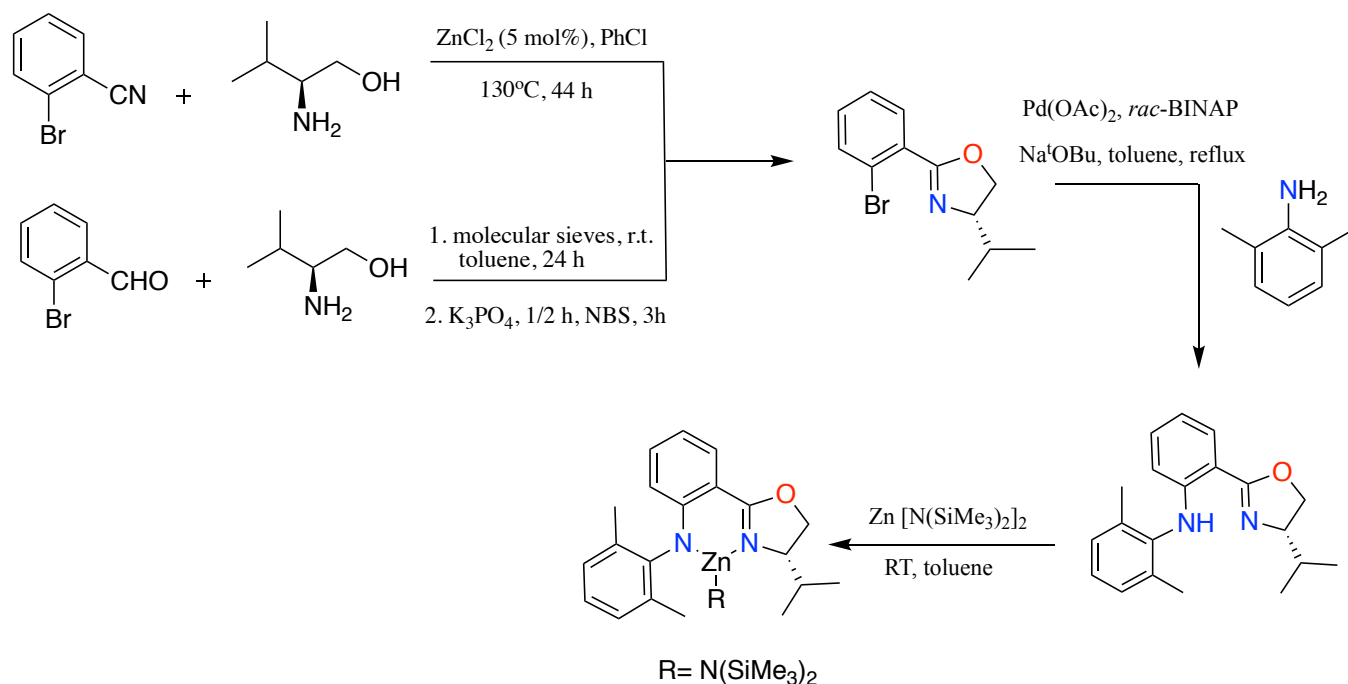
### 2.2.2 Synthesis of the Zinc Complex

Chiral 2-(2'-bromophenyl)-4-isopropylloxazole was first synthesized from reacting chiral amino alcohol (L-Valinol) with either 2-bromobenzonitrile or 2-bromobenzaldehyde in a one-step via two pathways (Scheme 1) according to previously published procedures.<sup>25</sup> In our hand, the first pathway tended to give purer product and better yields though the reaction time was longer. Then, the chiral (4*S*)-4,5-dihydro-2-[2'-(2,6-dimethylanilino)phenyl]-4-isopropylloxazole ligand was prepared via a palladium-catalyzed Buchwald-Hartwig amination reaction. The reaction was carried out by mixing the chiral oxazoline complex (1 equiv) and 2,6-dimethylaniline (1.2 equiv) in the presence of catalytic amounts of Pd(OAc)<sub>2</sub> (5 mol%) *rac*-BINAP (5 mol%) and *t*-BuONa (1.4 equiv) under refluxing toluene at 120 °C, yielding 80 % after purification by column chromatography. The amido-oxazolate zinc complex (catalyst **1**) was prepared by treatment of the obtained ligand with 1 equivalent of Zn[N(SiMe<sub>3</sub>)<sub>2</sub>]<sub>2</sub> in dry toluene. The reaction mixture was allowed to stir at room temperature for overnight. at room temperature (Scheme 1). The mixture was filtered and washed with hexane to afford a greenish-yellow product in high yields.

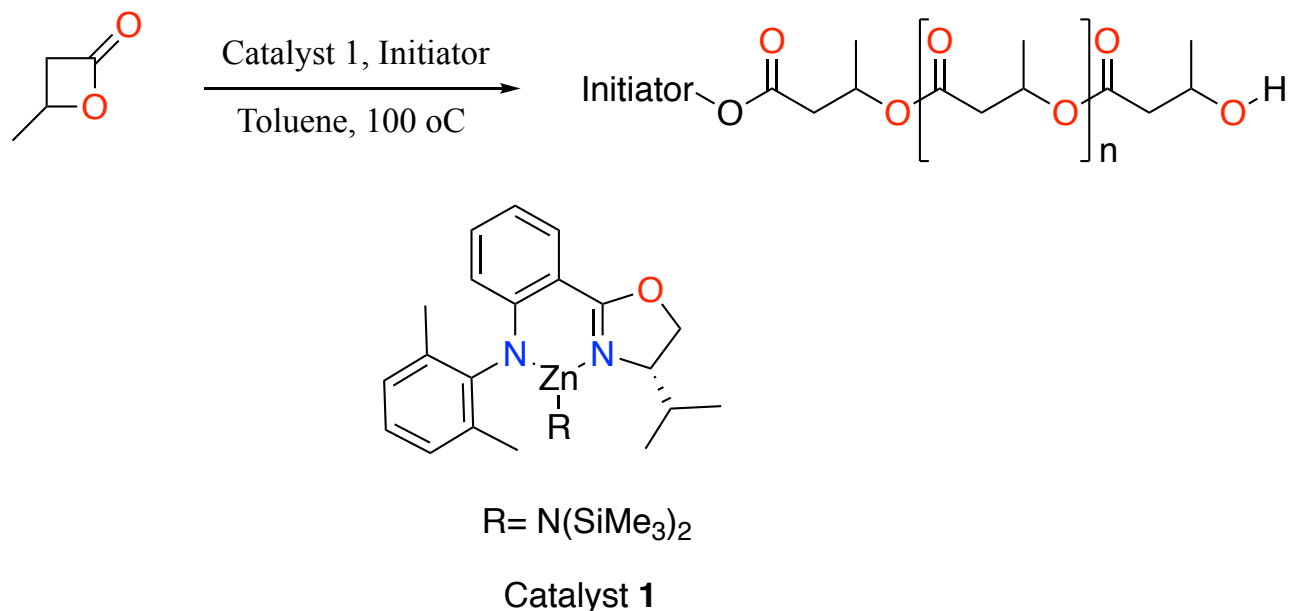
### 2.2.3 General Procedure for ROP of BBL

All reactions were performed under an inert atmosphere. In a glovebox under nitrogen, an oven-dried 10 mL Schlenk flask with a stir bar was charged with zinc catalyst (3 equiv, based on the arm's number), initiator (1 equiv), BBL (300 equiv, [100 equiv × arm's number]), and toluene (4.0 mL) (Scheme 2). The flask was capped and taken out, and then heated in an oil bath at 100 °C

until the complete conversion of BBL was observed by  $^1\text{H}$ -NMR spectroscopy. After evacuation of the volatile components, the resulting polymer was dissolved in DCM (1–3 mL), followed by addition of hexane (4–5 mL). The precipitation of the polymeric products was facilitated by cooling the flask briefly in liquid nitrogen, and the supernatant was decanted. After purification, the polymer was dried in a vacuum to constant weight to determine the yield and characterized by various NMR techniques, GPC, and DSC.



**Scheme 1.** Chiral Amido-Oxazolate Zinc Complex (Catalyst 1).



**Scheme 2.** Synthetic route of various-armed star-shaped PHBs.

**Poly(hydroxybutyrate) with Glycerin as an Initiator**, (90% yield),  $^1\text{H-NMR}$  (500 MHz,  $\text{CDCl}_3$ , 298 K):  $\delta$  5.23 (m,  $\text{CH}_3\text{CHCH}_2$ , 1H), 4.30 (m,  $\text{CH}_2\text{CHCH}_2$ , 1H), 4.17 (m,  $\text{CH}_3\text{CHCH}_2$ , 1H), 4.12 (d,  $\text{CH}_2\text{CHCH}_2$ , 4H), 3.12 (s,  $\text{CHOH}$ , 1H), 2.59 (d,  $\text{CH}_3\text{CHCH}_2$ , 2H), 2.47 (d,  $\text{CH}_3\text{CHCH}_2$ , 2H), 1.26 (d,  $\text{CH}_3\text{CHCH}_2$ , 3H), 1.21 (d,  $\text{CH}_3\text{CHCH}_2$ , 3H).  $^{13}\text{C-NMR}$  ( $\text{CDCl}_3$ , 298 K):  $\delta$  171.12 ( $\text{C=O}$ ), 168.25 ( $\text{C=O}$ ), 168.16 ( $\text{C=O}$ ), 68.26 ( $\text{CH}_2\text{CHCH}_2$ ), 66.65 ( $\text{CH}_3\text{CHCH}_2$ ), 63.41 ( $\text{CH}_3\text{CHCH}_2$ ), 61.29 ( $\text{CH}_2\text{CHCH}_2$ ), 42.34 ( $\text{CH}_3\text{CHCH}_2$ ), 39.77 ( $\text{CH}_3\text{CHCH}_2$ ), 21.53 ( $\text{CH}_3\text{CHCH}_2$ ), 18.79 ( $\text{CH}_3\text{CHCH}_2$ ).

**Poly(hydroxybutyrate) with Pentaerythritol as Initiator**, (88% yield),  $^1\text{H-NMR}$  (500 MHz,  $\text{CDCl}_3$ , 298 K):  $\delta$  5.23 (m,  $\text{CH}_3\text{CHCH}_2$ , 1H), 4.17 (m,  $\text{CH}_3\text{CHCH}_2$ , 1H), 4.09 (s,  $\text{C}(\text{CH}_2)_4$ , 8H), 3.09 (s,  $\text{CHOH}$ , 1H), 2.59 (d,  $\text{CH}_3\text{CHCH}_2$ , 2H), 2.45 (d,  $\text{CH}_3\text{CHCH}_2$ , 2H), 1.26 (d,  $\text{CH}_3\text{CHCH}_2$ , 3H), 1.14 (d,  $\text{CH}_3\text{CHCH}_2$ , 3H).  $^{13}\text{C-NMR}$  ( $\text{CDCl}_3$ , 298 K):  $\delta$  171.98 ( $\text{C=O}$ ), 169.64



(C=O), 169.32 (C=O), 67.75 (CH<sub>3</sub>CHCH<sub>2</sub>), 64.45 (CH<sub>3</sub>CHCH<sub>2</sub>), 62.30 (C(CH<sub>2</sub>)<sub>4</sub>), 43.52 (C(CH<sub>2</sub>)<sub>4</sub>), 43.38 (CH<sub>3</sub>CHCH<sub>2</sub>), 40.88 (CH<sub>3</sub>CHCH<sub>2</sub>), 22.50 (CH<sub>3</sub>CHCH<sub>2</sub>), 19.86 (CH<sub>3</sub>CHCH<sub>2</sub>).

**Poly(hydroxybutyrate) with MSSP as Initiator**, (89% yield), <sup>1</sup>H-NMR (500 MHz, CDCl<sub>3</sub>, 298 K): δ 5.24 (m, CH<sub>3</sub>CHCH<sub>2</sub>, 1H), 5.09 and 4.96 (*sucrose*), 4.26 (t, CH<sub>3</sub>OCHCH<sub>2</sub>, 1H), 4.18 (m, CH<sub>3</sub>CHCH<sub>2</sub>, 1H), 3.38 (s, CH<sub>3</sub>OCHCH<sub>2</sub>, 3H), 3.17 (t, CH<sub>3</sub>OCHCH<sub>2</sub>, 1H), 3.10 (s, CHOH, 1H), 2.60 (d, CH<sub>3</sub>CHCH<sub>2</sub>, 2H), 2.45 (d, CH<sub>3</sub>CHCH<sub>2</sub>, 2H), 2.11 (t, COCH<sub>2</sub>CH<sub>2</sub>, 2H), 1.86 (t, CHCH<sub>2</sub>CH, 2H), 1.72 (m, COCH<sub>2</sub>CH<sub>2</sub>, 2H), 1.58 (m, CHCH<sub>2</sub>(CH<sub>2</sub>)<sub>2</sub>CH<sub>2</sub>CH<sub>3</sub>, 2H), 1.58 (m, CHCH<sub>2</sub>(CH<sub>2</sub>)<sub>2</sub>CH<sub>2</sub>CH<sub>3</sub>, 2H), 1.39 (m, CHCH<sub>2</sub>(CH<sub>2</sub>)<sub>2</sub>CH<sub>2</sub>CH<sub>3</sub>, 2H), 1.25 (d, CH<sub>3</sub>CHCH<sub>2</sub>, 3H), 1.14 (d, CH<sub>3</sub>CHCH<sub>2</sub>, 3H), 0.87 (d, CHCH<sub>2</sub>(CH<sub>2</sub>)<sub>2</sub>CH<sub>2</sub>CH<sub>3</sub>, 23H),

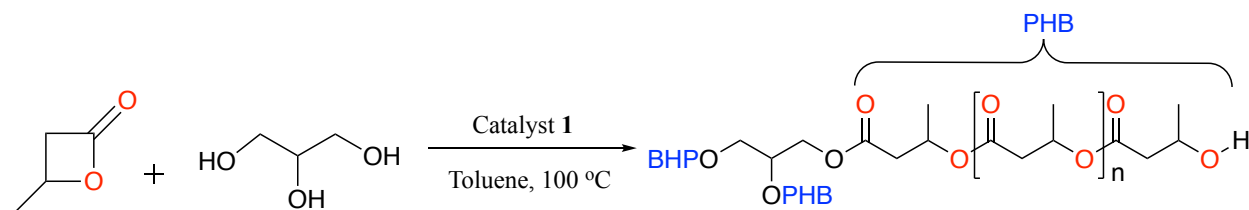
**Poly(hydroxybutyrate) with HSSP as Initiator**, (78% yield), <sup>1</sup>H-NMR (500 MHz, CDCl<sub>3</sub>, 298 K): δ 5.23 (m, CH<sub>3</sub>CHCH<sub>2</sub>, 1H), 5.07 and 4.96 (*sucrose*), 4.17 (m, CH<sub>3</sub>CHCH<sub>2</sub>, 1H), 3.85 (m, CH<sub>2</sub>(CH)<sub>2</sub>CH<sub>2</sub>, 1H), 3.17 (s, CHOH, 1H), 2.58 (d, CH<sub>3</sub>CHCH<sub>2</sub>, 2H), 2.45 (d, CH<sub>3</sub>CHCH<sub>2</sub>, 2H), 1.99 (t, COCH<sub>2</sub>CH<sub>2</sub>, 2H), 1.84 (t, CHCH<sub>2</sub>CH, 2H), 1.57 (m, COCH<sub>2</sub>CH<sub>2</sub>, 2H), 1.48 (m, CHCH<sub>2</sub>(CH<sub>2</sub>)<sub>2</sub>CH<sub>2</sub>CH<sub>3</sub>, 2H), 1.48 (m, CHCH<sub>2</sub>(CH<sub>2</sub>)<sub>2</sub>CH<sub>2</sub>CH<sub>3</sub>, 2H), 1.39 (m, CHCH<sub>2</sub>(CH<sub>2</sub>)<sub>2</sub>CH<sub>2</sub>CH<sub>3</sub>, 2H), 1.26 (d, CH<sub>3</sub>CHCH<sub>2</sub>, 3H), 1.14 (d, CH<sub>3</sub>CHCH<sub>2</sub>, 3H), 0.85 (d, CHCH<sub>2</sub>(CH<sub>2</sub>)<sub>2</sub>CH<sub>2</sub>CH<sub>3</sub>, 3H).

## 2.3 Results and Discussion

### 2.3.1 ROP of BBL with Glycerin

A three-armed star-shaped PHB having hydroxyl end groups was first synthesized by ROP of BBL initiated from glycerin as the tri-functional initiator in toluene at 100 °C with catalyst **1** (Scheme 3). The corresponding data of ROP of *rac*-β-butyrolactone (BBL) at different conditions are summarized in Table 1. As shown in Table 1, 100 % of monomer conversion was achieved within 60–90 minutes when the reaction was performed at different concentrations. Good

agreement between experimental and calculated molecular weights ( $M_n$  up to 103400 g/mol) were obtained (Table 1, entries 1–4). Up to 20 equivalent of glycerin ratio can be applied, whereas treatment with higher amount of glycerin resulted in the decomposition of the catalyst (Table 1, entries 5–6).



**Scheme 3.** Synthesis of 3-armed star-shaped polymers.

**Table 1.** ROP of *rac*- $\beta$ -butyrolactone using catalyst **1** with glycerin.<sup>a</sup>

Entry	Zn/Gly/BBL	Time	$M_n(\text{Calcd})^b$	$M_n(\text{NMR})^c$	Yield % <sup>d</sup>	Conv%
1	3:1:30	60 min	2675	2743	78	100
2	3:1:300	60 min	25919	25257	82	100
3	3:1:600	80 min	51746	60355	86	100
4	3:1:1200	90 min	103400	104526	90	100
5	3:10:600	80 min	5257	6549	88	100
6	3:20:600	90 min	2675	2933	84	100

<sup>a</sup>Polymerizations were run in toluene at 100 °C. The reactions were monitored by NMR until all BBL was consumed. <sup>b</sup>Calculated on the basis of conversion and catalyst/initiator loading. <sup>c</sup>Determined by the end-group/main-chain ratio in <sup>1</sup>H-NMR. <sup>d</sup>Isolated yields.

The microstructure of the obtained PHBs with glycerin as a central core was further confirmed by NMR spectroscopic techniques. Figure 1 shows a typical <sup>1</sup>H-NMR spectrum of the PHB obtained with a ratio of [Zn]/[Glycerin]/[BBL] = 3:10:600 (entry 5 in Table 1). The strong

signal (peak **e**) of the methine protons corresponding to the main chain repeating butyrate units was appeared at 5.23 ppm, and the other strong peaks **d** and **f** at 2.59-2.47 ppm and 1.26 ppm were assigned to the methylene and methyl protons, respectively. A weak yet singlet peak **h** at 4.17 ppm was attributed to the methine protons adjacent to terminal OH group, and the methylene and methyl protons (peak **g** and **i**) of the terminal repeating butyrate units were overlapped with the large main chain signals (peaks **d** and **f**). In addition, the chain end hydroxyl protons appeared as a doublet at 3.12 ppm, whereas another end of the chain was characterized by glycerin protons. The peaks **a** and **b** at 4.12 ppm and 4.29 ppm could be assigned to the methylene and methine protons of glycerin, which supported glycerin was incorporated into the polymer structure as the central core. The structure was also confirmed by  $^{13}\text{C}$ -NMR spectroscopy (Figure 2). The presences of the main chain and the chain end of PHBs resonances peaks were observed, as reported previously.<sup>23</sup> Besides the main chain carbons, the peaks **a** and **b** at 61.29 and 68.26 ppm could be assigned to methylene and methine carbons of the glycerin, respectively. Additionally, the presences of the polymer chain and the glycerin core was also verified by  $^1\text{H}$ - $^{13}\text{C}$  COSY (HETCOR) NMR spectrum. As shown in Figure 3, a correlation between the methylene proton and carbon of glycerin group was occurred. The existence of the characteristic peaks of the initiator and PHB indicates that three-hydroxyl groups of glycerin effectively initiated ROP of BBL as the star core with PHB arms.

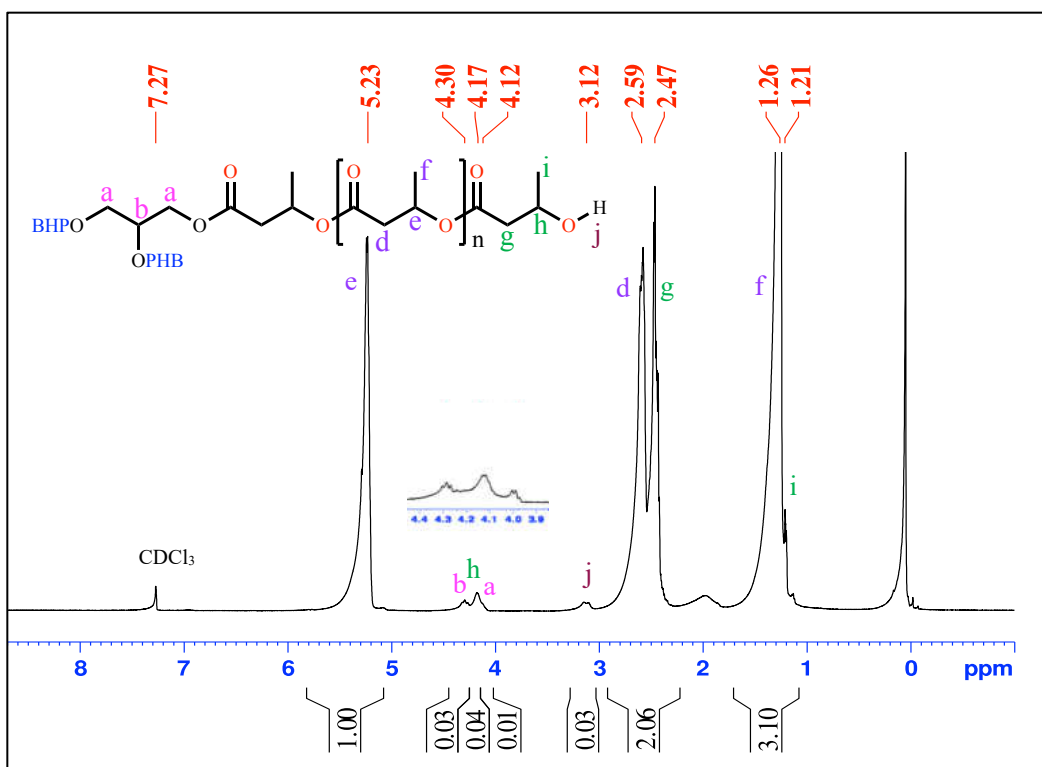


**Figure 1.** <sup>1</sup>H-NMR spectrum of the PHB with glycerin as a central core.

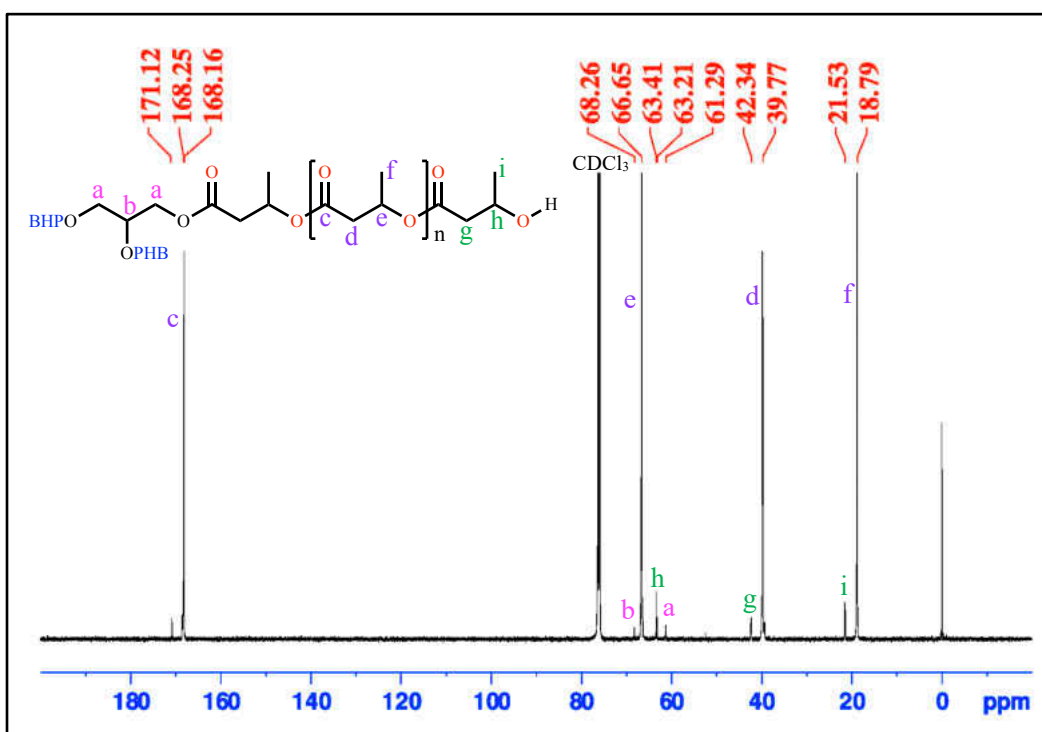


**Figure 2.** <sup>13</sup>C-NMR spectrum of the PHB with glycerin as a central core.

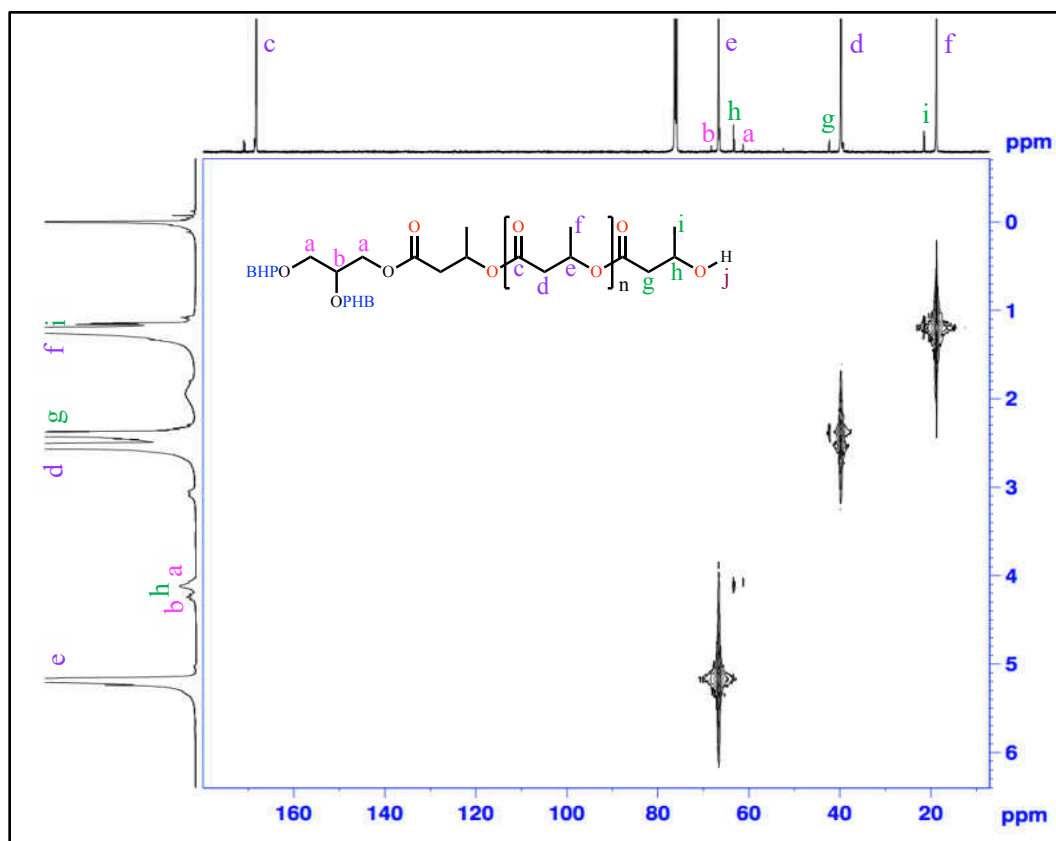
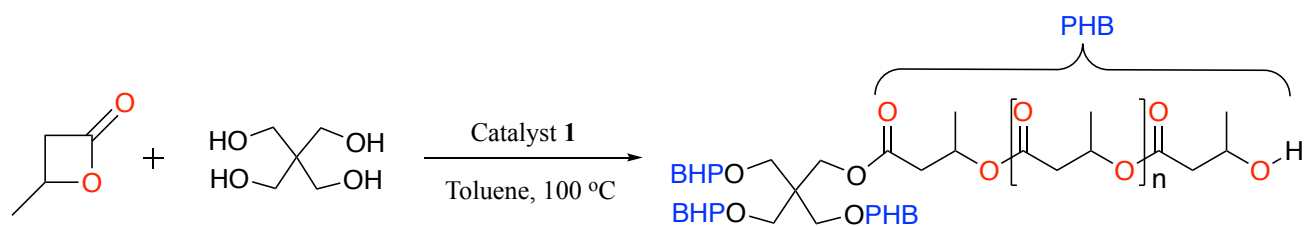


**Figure 3.**  $^1\text{H}$ - $^{13}\text{C}$  COSY NMR spectrum of the PHB with glycerol as a central core.

### 2.3.2 ROP of BBL with Pentaerythritol

Four-armed star-shaped PHBs were prepared following a similar one-step synthetic procedure. Thus, pentaerythritol (PE) was used as a tetra-functional initiator, whereas the hydroxyl end groups of the PE core subsequently initiated ROP of BBL as shown in Scheme 4, and the results are summarized in Table 2. In most cases 100% conversions were achieved within 60 minutes, and the resulting PHBs were largely atactic, as determined by IG- $^{13}\text{C}$  NMR. It was observed that a decent agreement between theoretical and experimental molecular weights, and narrow dispersities (1.15–1.34) were obtained. Furthermore, up to 10 equivalents of PE (vs catalyst) could be employed and the molecular weights of the polymers could be controlled by changing the Zn/alcohol ratios, indicating that alcohols also acted as chain transfer agents in the

reaction. Higher loading of alcohol (>10 equivalents) resulted in the decomposition of zinc catalyst and loss of the ROP activity.



**Scheme 4.** Synthesis of 4-armed star-shaped polymers.

**Table 2.** ROP of *rac*-β-butyrolactone using catalyst **1** with pentaerythritol.<sup>a</sup>

Entry	Zn/PE/BBL	Time	$M_n(\text{Calcd})^b$	$M_n(\text{NMR})^c$	$M_n(\text{GPC})^d$	$\bar{D}^d$	Yield % <sup>e</sup>	Conv%
1	4:1:40	60 min	3580	3407	1406	1.20	68	100
2	4:1:100	60 min	8745	9526	2443	1.32	75	100
3	4:1:400	60 min	34572	42567	14256	3.07	84	100
4	4:1:800	90 min	69008	69107	24984	1.34	88	100
5	4:10:800	4 h	7023	17353	15852	1.15	86	100
6	4:50:800	3h	1514	996	---	---	67	100

<sup>a</sup>Polymerizations were run in toluene at 100 °C. The reactions were monitored by NMR until all BBL was consumed. <sup>b</sup>Calculated on the basis of conversion and catalyst/initiator loading. <sup>c</sup>Determined by the end group/main chain ratio in <sup>1</sup>H-NMR. <sup>d</sup>Determined by gel permeation chromatography calibrated with polystyrene standards in THF. <sup>e</sup>Isolated yields.

A conversion-time profile of four-armed PHBs formation is shown in Figure 4. As shown in the figure, the conversion of BBL monomer increased rapidly and reached full conversion in relatively short times. From the plot, it was established that the initiation was instantaneously, and all arms of the initiator participated in the initiating chain growth. The number-average molecular

weight ( $M_n$ ) of the resulting polymer increased linearly with the conversion, and the dispersity was extremely narrow. In addition, the plot of  $-\ln([M]/[M]_0)$  against the reaction time ( $t$ ) for polymerization initiated with PE initiator, where  $[M]_0$  is the initial monomer concentration and  $[M]$  is the monomer concentration at reaction time, gave a straight line at least up to 99% monomer conversion (Figure 5). This result demonstrated that the initiation step was fast, and the number of propagation chains remained constant throughout the reaction.<sup>13</sup>

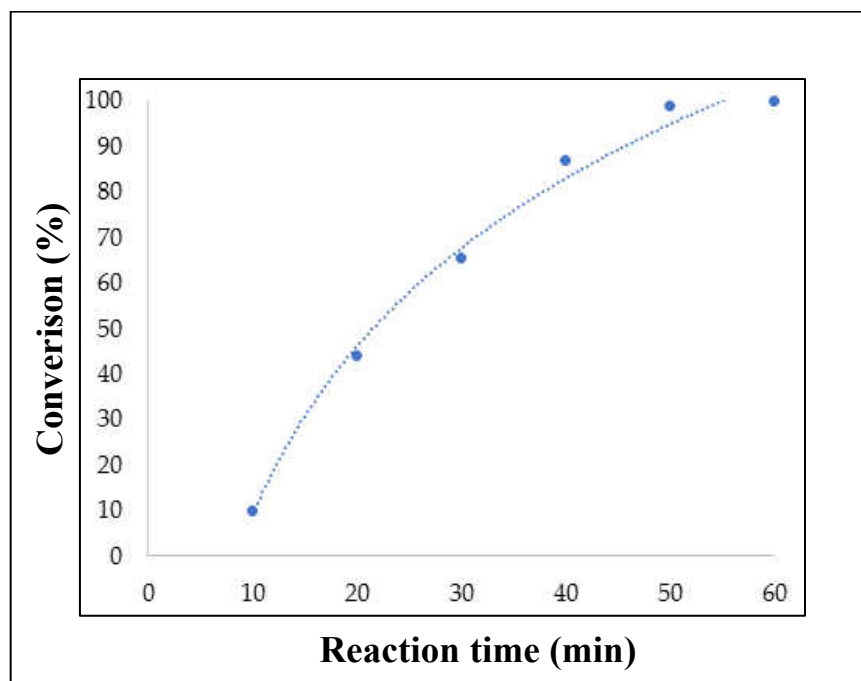


**Figure 4.** Conversion as a function of reaction time for the polymerization of BBL with PE in toluene,  $T = 100\text{ }^{\circ}\text{C}$ . Polymerization was initiated with catalyst **1**. [catalyst **1**]:[PE]:[BBL] = 4:1:800.

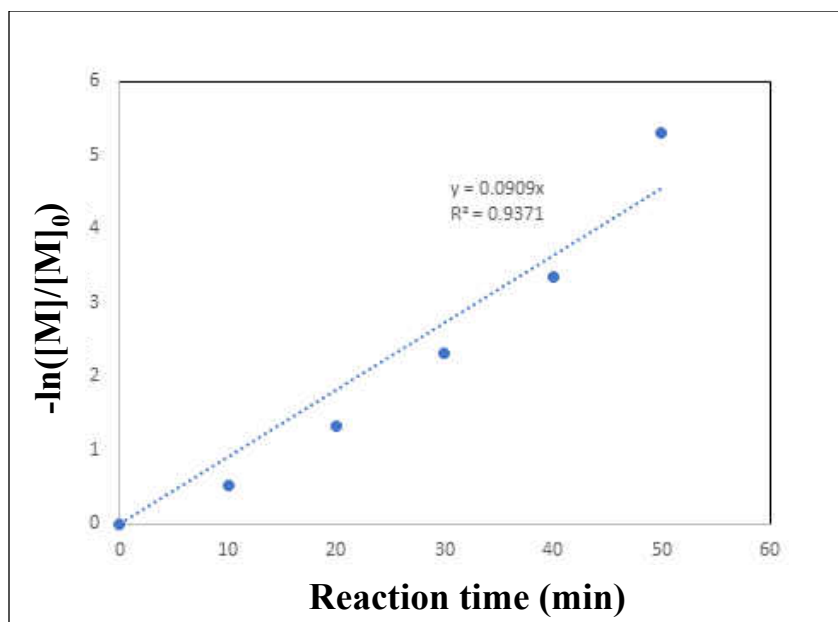


**Figure 5.** Plot of BBL monomer conversion expressed as  $-\ln([M]/[M]_0)$  versus reaction time for polymerization initiated with PE initiator,  $[M]/[I] = 400$ , as monitored by  $^1\text{H}$ -NMR spectroscopy in  $\text{CDCl}_3$ .

Figure 6 shows the  $^1\text{H}$ -NMR spectrum of the star-shaped PHB prepared with pentaerythritol (PE) as a core. The  $^1\text{H}$ -NMR analysis of a representative sample ( $[\text{Zn}]/[\text{PE}]/[\text{BBL}] = 4:1:400$ ) revealed the presence of methylene resonance at 4.09 ppm (peak **a**) corresponding to the PE moiety, whereas the chain end was characterized by a terminal hydroxybutyrate unit featuring a singlet at 4.17 ppm (peak **h**) for the methine protons and a doublet at 3.09 ppm for hydroxyl protons (peak **j**), which confirmed the presence of PE as the central core. The diastereotopic methylene protons of the PHB (peak **d**) were seen at 2.59 and 2.45 ppm. The peaks at 5.23 and 1.26 ppm were assigned to methine and methyl protons, respectively. The ratio of the integrations of the hydroxyl (3.09 ppm) vs methylene of PE (4.09 ppm) protons was 4:8, in agreement with them being the four ends of the chain. In addition, the 3.09 ppm signal showed no



correlation with  $^{13}\text{C}$ - signals in the  $^1\text{H}$ - $^{13}\text{C}$  HETCOR NMR spectrum shown in Figure 7 and 8. The presence of the PE core was also supported by the  $^{13}\text{C}$ -NMR spectrum. Together, these observations support that the PE unit is incorporated into the core and the polymer end groups are hydroxybutyrate.

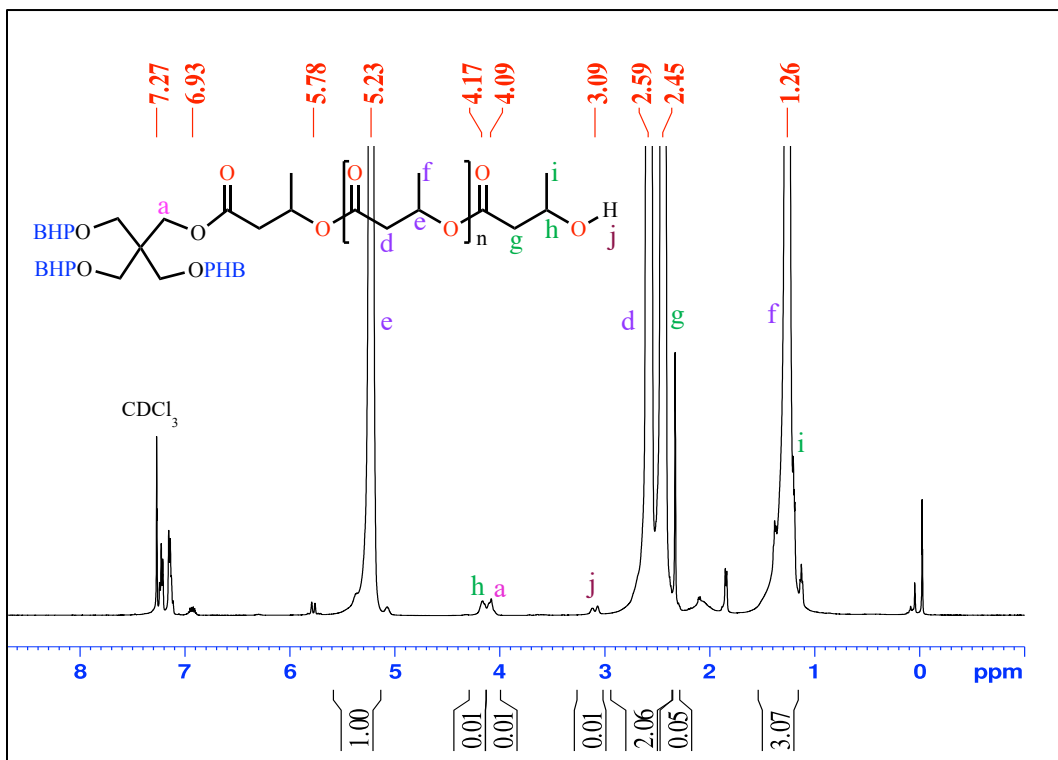


**Figure 6.**  $^1\text{H}$ -NMR spectrum of the PHB with pentaerythritol as a central core.

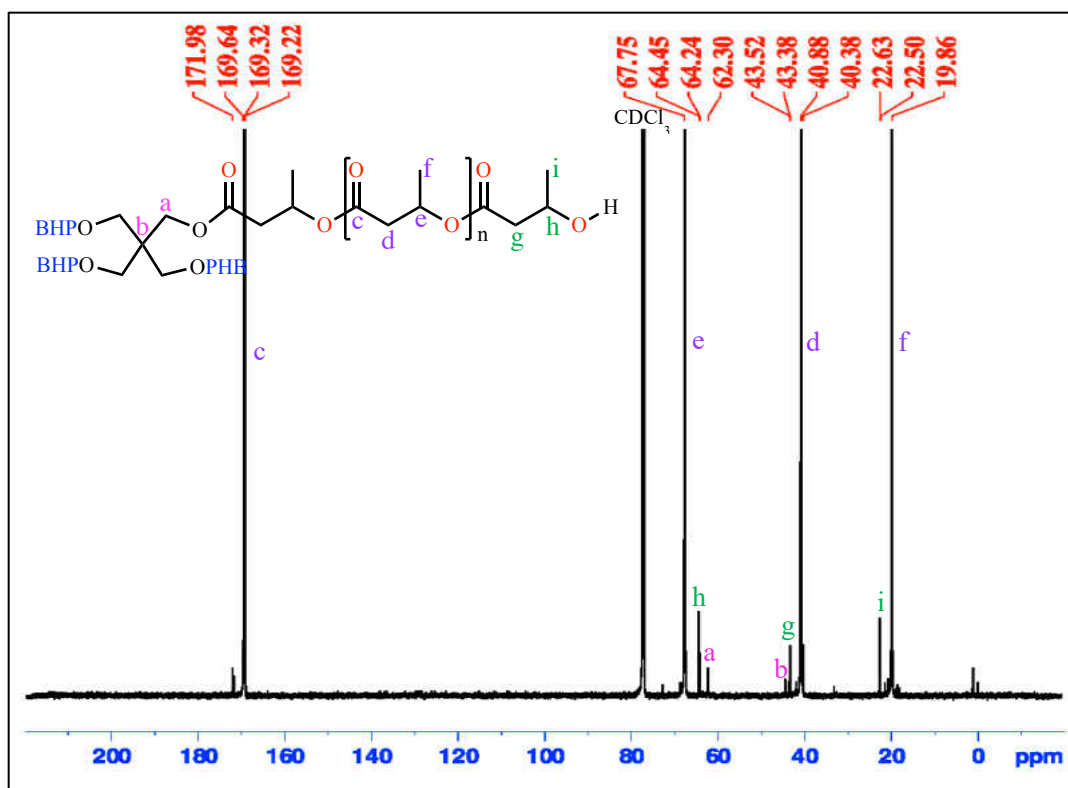


**Figure 7.**  $^{13}\text{C}$ -NMR spectrum of the PHB with pentaerythritol as a central core.

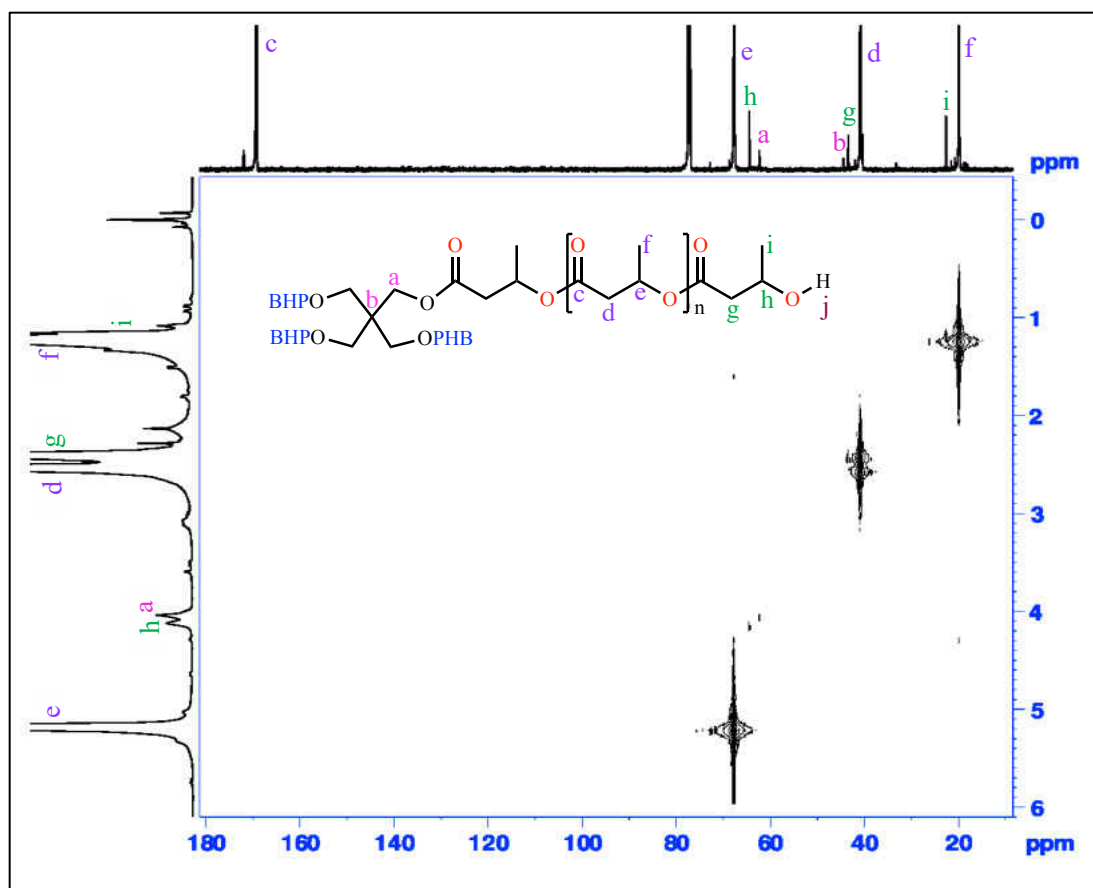


**Figure 8.**  $^1\text{H}$ - $^{13}\text{C}$  COSYNMR spectrum of the PHB with pentaerythritol as a central core.

### 2.3.3 ROP of BBL with Polyols

Beside the glycerin and PE cores, branched methoxylated sucrose soyate polyol (MSSP) and hydroxylated sucrose soyate polyol (HSSP), considered as highly functional bio-based polyols (Figure 9), were used as the macromolecular initiators for the ROP of BBL to obtain the star-shaped and highly branched PHBs. It has been shown that introducing biobased polyols such as sucrose esters could give polyurethanes higher modulus, hardness, and glass transition temperatures ( $T_g$ ) compared to other biobased and petroleum-based polyols.<sup>24,26-28</sup> Herein, we showed that these polyols can act as a central core to create a well-fashioned star polyester.

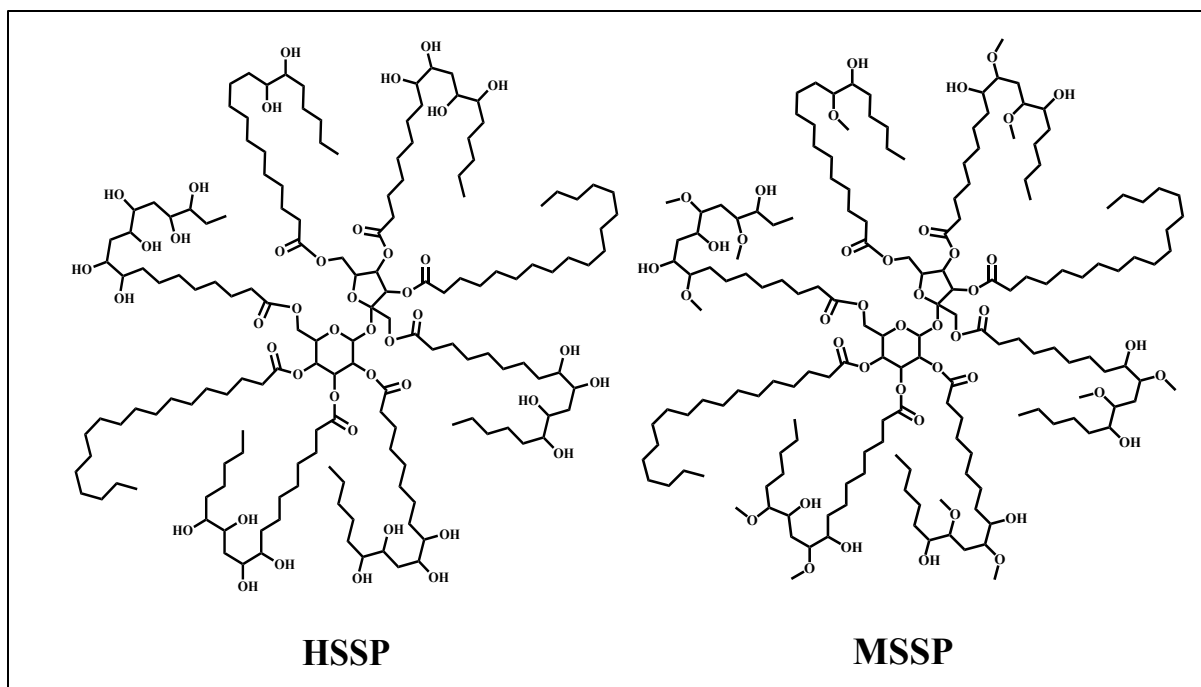
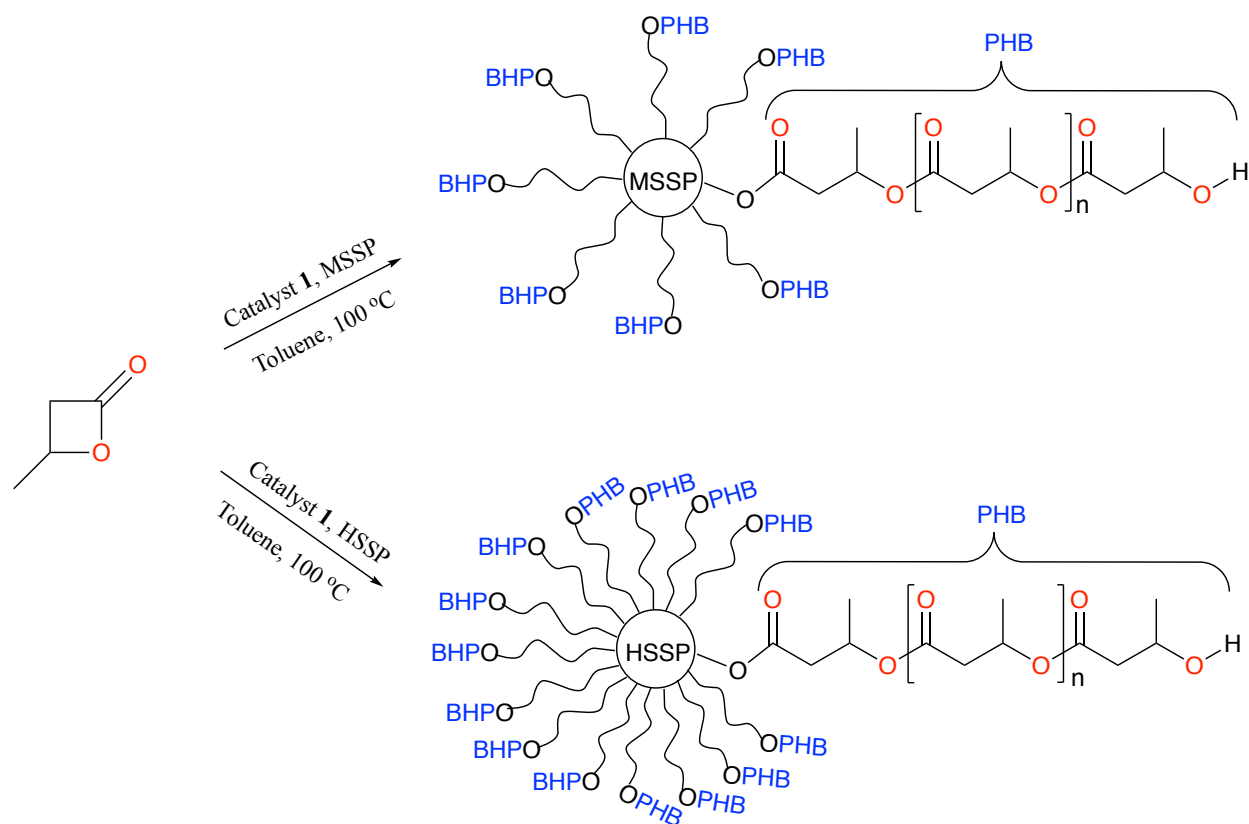


**Figure 9.** Molecular structure of the MSSP and HSSP core initiators.

The polymerization of BBL was carried out with MSSP in the presence of catalyst **1** in toluene at 100 °C as shown in Scheme 5. The results of the polymerization using different amount of BBL monomer are presented in Table 3. BBL in most of the reactions was completely consumed within 60 minutes, and the yields of the polymers were above 80 % (Table 3, entries 1–4). However, the resultant molecular weight of the polymer was smaller than the calculated molecular weight. The dispersities ( $\bar{M}_w/\bar{M}_n = 1.09\text{--}1.87$ ) were relatively broad. These results showed that the use of MSSP as the core initiator for the synthesis of star-shaped PHBs via ROP was successful.



**Scheme 5.** Synthesis of star-shaped and highly branched PHBs the presence of MSSP and HSSP.

**Table 3.** ROP of *rac*- $\beta$ -butyrolactone using catalyst **1** with MSSP and HSSP.<sup>a</sup>

Entry	Zn/I/BBL	Time	$M_n(\text{Calcd})^b$	$M_n(\text{NMR})^c$	$M_n(\text{GPC})^d$	$\bar{D}^d$	Yield % <sup>e</sup>	Conv%
1	12:1:120	60 min	13355	9050	9314	1.20	58	100
2	12:1:1200	60 min	106332	35448	38391	1.78	74	90
3	12:1:2400	60 min	209640	169880	132771 16357	1.27 1.09	82	100
4	12:1:4800	90 min	416256	38480	24984	1.25	89	100
5 <sup>f</sup>	24:1:240	60 min	23583	8761	---	---	67	100
6 <sup>f</sup>	24:1:2400	180 min	209538	71794	---	---	78	100

<sup>a</sup>Polymerizations were run in toluene at 100 °C. The reactions were monitored by NMR until all BBL was consumed. <sup>b</sup>Calculated on the basis of conversion and catalyst/initiator loading. <sup>c</sup>Determined by the end group/main chain ratio in <sup>1</sup>H-NMR. <sup>d</sup>Determined by gel permeation chromatography calibrated with polystyrene standards in THF. <sup>e</sup>Isolated yields. <sup>f</sup>HSSP was used as the core.

A representative <sup>1</sup>H-NMR spectrum of the star-shaped PHBs obtained with MSSP as a central core is shown in Figure 10. Besides the main chain signals of the hydroxybutyrate at 1.26, 2.45 and 2.59, and 5.25 ppm (peak **f**, **d**, and **e**, respectively) and the methine protons of the chain end at 4.18 ppm, there are additional signals that match the MSSP core peaks. For instance, the peak at 3.38 ppm (peak **o**) can be assigned to the methoxy protons of the central core, the protons with the chemical shift at 3.17 ppm can be assigned to the methine protons (peak **m**) in the  $\alpha$  position of the methoxy groups whereas the other methine protons (peak **m'**) near the oxygen atom of the hydroxybutyrate groups show signals at 4.26 ppm, and the protons of the hydroxyl group in the end chain appear at 3.10 ppm (peak **j**). Moreover, the triplet signal (peak **a**) at 0.87 ppm corresponds to the terminal methyl protons of the MSSP core. The backbone methylene protons (peak **k**) in MSSP overlapped with the methyl protons in the PHB main chain and appeared at 1.26 ppm. This demonstrates that the MSSP had been incorporated with the hydroxybutyrate to form the star-shaped PHBs.

In a similar manner, highly branched PHBs were synthesized by ROP in the presence of catalyst **1** and HSSP as the core initiator (Scheme 5). The results are presented in Table 3 (entry 5 and 6), and polymers with higher arm numbers and different chain lengths could be obtained in good yields and low dispersity. Additionally, the resultant molecular weights by GPC were smaller

than molecular weights calculated from conversion and catalyst loading. This can be attributed to the smaller hydrodynamic volume of star-shaped and branched macromolecules.<sup>29, 30</sup>

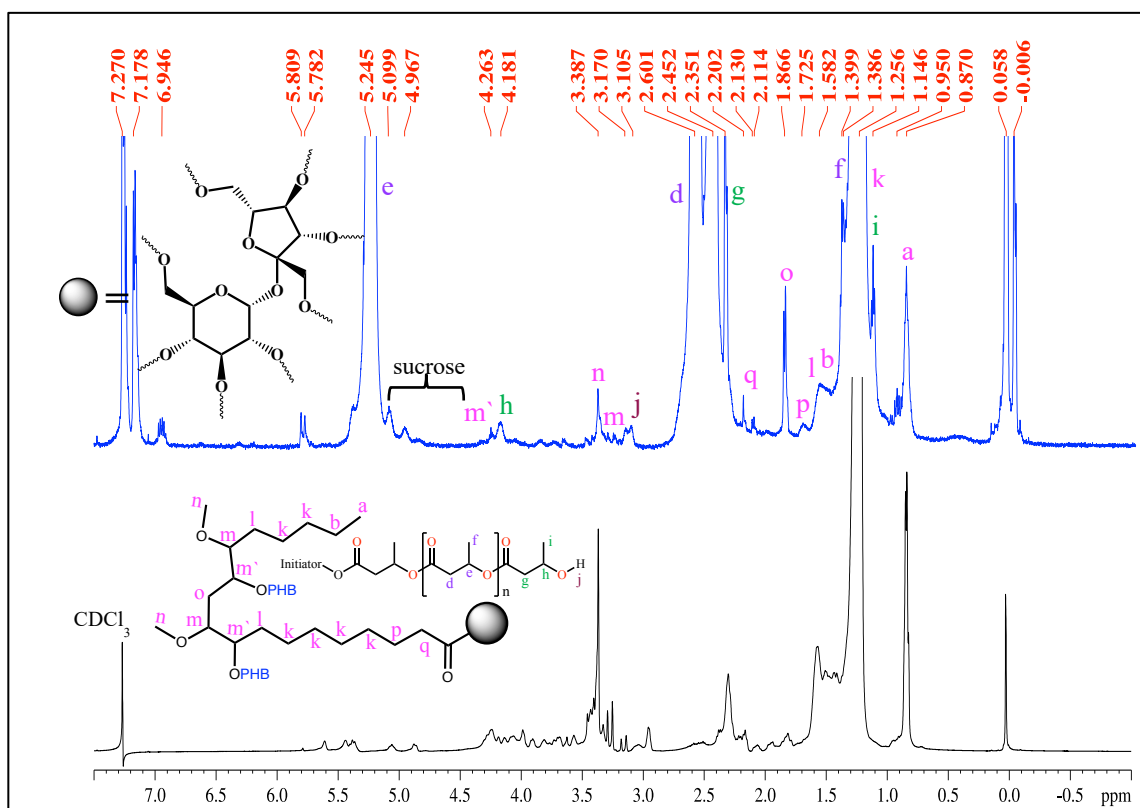


**Figure 10.** <sup>1</sup>H-NMR spectrum of the PHB with MSSP as a central core in CDCl<sub>3</sub>: MSSP core (bottom), and [M]/[I] = 4800 (Table 3, entry 4) (top).

Figure 11 shows a typical <sup>1</sup>H-NMR spectrum of the star-shaped PHBs synthesized with HSSP. The resonance peaks of the hydroxybutyrate repeating units of PHBs and the HSSP core, were clearly observed. The presence of resonances of HSSP protons indicated the occurrence of the polymerization initiated with HSSP as a central core for the formation of highly branched PHBs. In addition to the characteristic signals of the sucrose soyate polyol backbone of the HSSP core, the protons (peak e) signal in the MSSP assigned to methoxy did not appear in the HSSP core. These results provide an excellent evidence for the formation of star-shaped and highly branched PHBs with the MSSP and HSSP core as a chain transfer agent for the ROP of BBL.

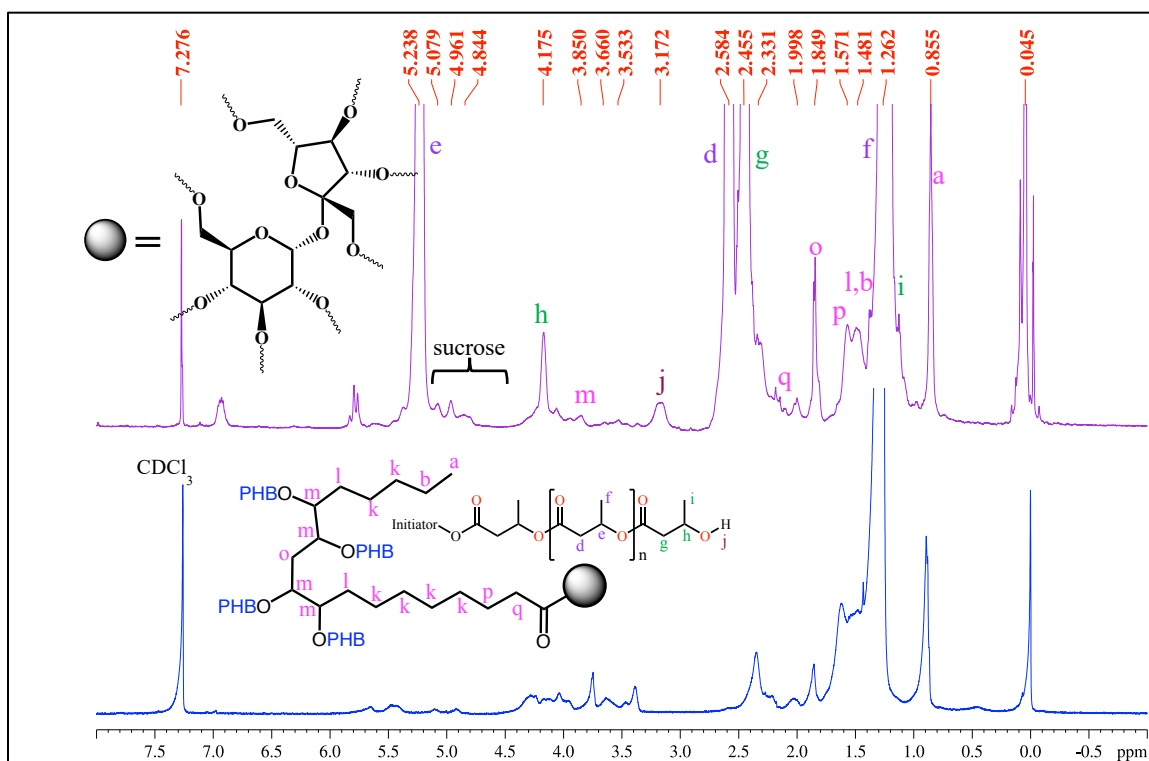


**Figure 11.**  $^1\text{H}$ -NMR spectrum of the PHB with HSSP as a central core in  $\text{CDCl}_3$ : HSSP core (bottom), and  $[\text{M}]/[\text{I}] = 2400$  (Table 3, entry 6) (top).

## 2.4 Thermal Properties

In order to study the effects of the arm number and arm length on thermal properties, differential scanning calorimetry (DSC) and thermogravimetric analysis (TGA) methods were conducted on the prepared star-shaped PHBs, and the characteristic results are summarized in Table 4. Commonly, star-shaped polymers with a higher arm number and arm length exhibit faster thermal decomposition and noticeably lower thermal transition when compared with their linear counterparts with the same monomer/initiator ratio.<sup>30</sup> With the use of the same monomer/initiator ratio, the glass transition temperature ( $T_g$ ) and the temperature of maximum decomposition rate ( $T_{\text{max}}$ ) of the star-shaped and highly branched PHBs decreased as either the arm numbers increased, or the arm lengths decreased.<sup>31,32</sup>



The glass transition temperature ( $T_g$ ) of the polymer is one of its essential properties, which is the temperature at which the polymer transitions from a hard and glassy material to a less rigid and more rubbery material.<sup>33</sup> The values of the glass transition temperatures ( $T_g$ s) obtained from the DSC thermograms of the star-shaped and highly branched PHBs are summarized in Table 4. As shown in Figure 12,  $T_g$  value was gradually shifted to lower temperatures as the arm numbers increased. The  $T_g$  values of PHB with glycerin and PE as a core were found to be comparable to that of PHB with highly branched initiator MSSP. For instance,  $T_g$  value of star-shaped PHB with glycerin as the central core was 8.0 °C, and when the arm numbers increased with the use of MSSP as a core for the highly branched PHBs, the  $T_g$  decreased to 1.4 °C. Indeed, PHB with MSSP as a core showed a slightly lower  $T_g$  value than the linear PHB. These results clearly demonstrate that arm number of the initiators can affect the  $T_g$  values. Furthermore, besides the arm number presented, the arm lengths could also play an important role in determining the  $T_g$  of PHBs. Herein, the  $T_g$  of the star-shaped and highly branched PHBs with the same arm numbers but different arm lengths, were investigated and exhibited lower  $T_g$  value when the arm lengths decreased, as shown in Figure 13-15. The results of the obtained PHBs are summarized in Table 5-7. These observations provide additional support that the thermal properties of PHBs could be modified by changing the arm number and arm length of PHBs.

**Table 4.** Thermal properties of star-shaped PHBs.<sup>a, b</sup>

Entry	[I]/[Zn]/[BBL]	$T_{-5\%}$	$T_{-50\%}$	$T_{-95\%}$	$T_{max}$	$T_g$
1	Glycerin	277	297	300	302	8.0
2	Pentaerythritol	279	294	296	300	7.6
3	MSSP	262	290	294	299	1.4

<sup>a</sup>Temperatures in °C. <sup>b</sup> $T_g$  values were determined from the second heating cycle in DSC.  $T_{-5\%}$ ,  $T_{-50\%}$ , and  $T_{-95\%}$  refer to the temperatures at which 5%, 50%, and 95% weight losses were observed in TGA, respectively.

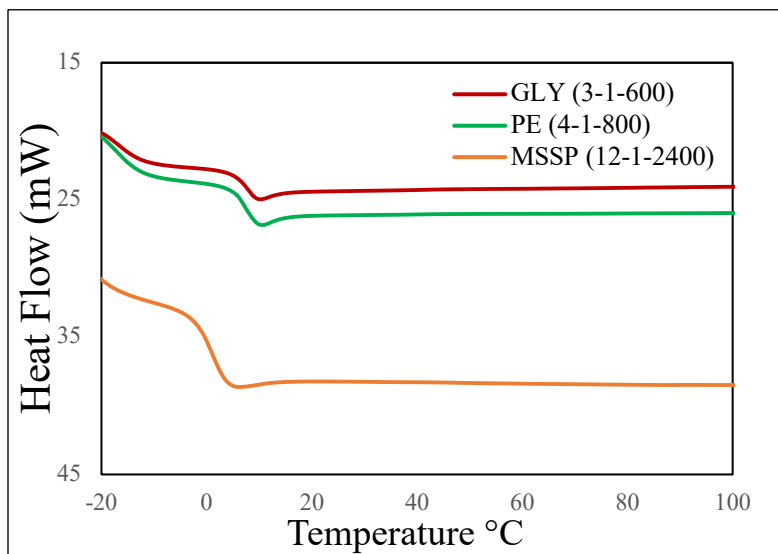


**Figure 12.** DSC analysis of star-shaped PHBs.

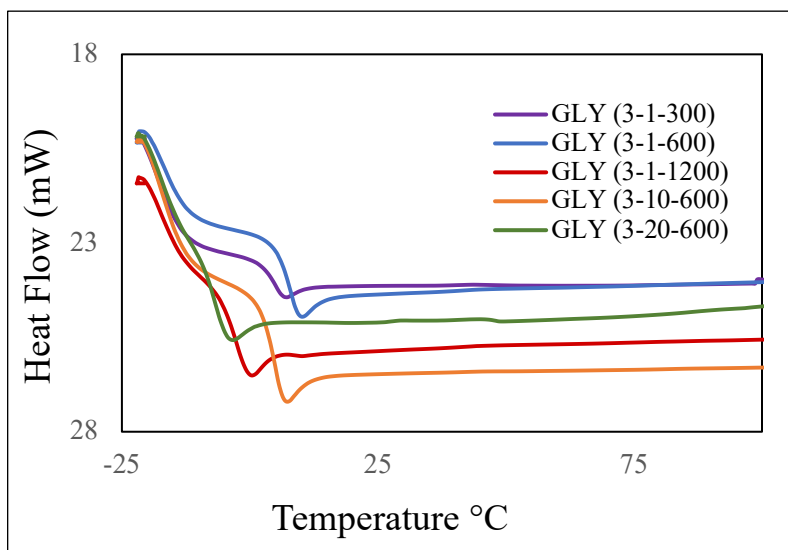


**Figure 13.** DSC analysis of star-shaped PHBs with glycerin with different arm lengths.

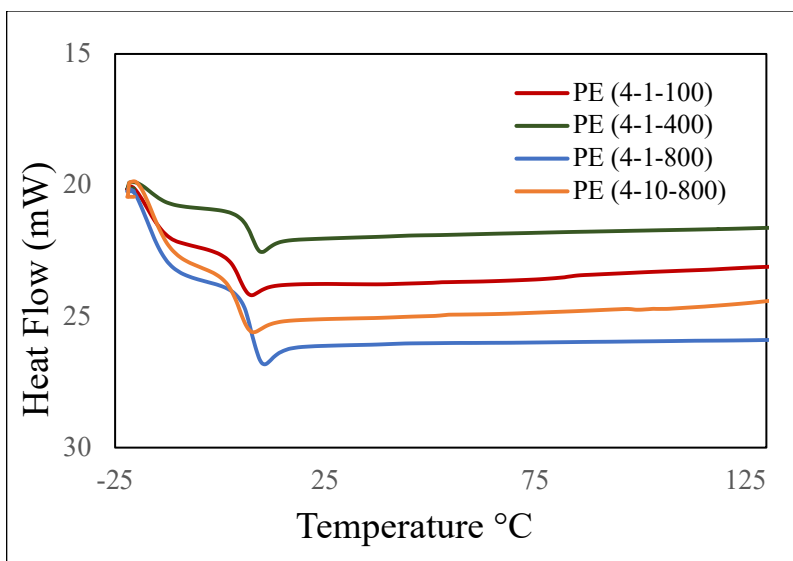


**Figure 14.** DSC analysis of star-shaped PHBs with PE with different arm lengths.

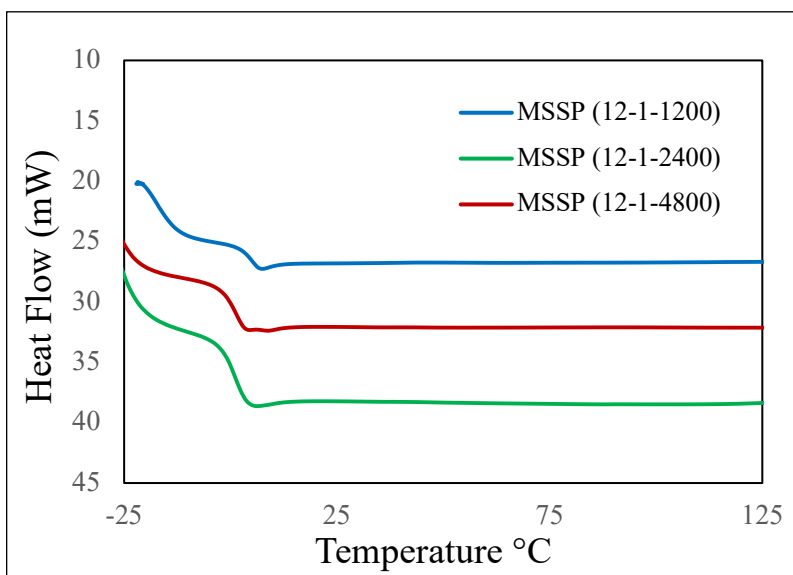


**Figure 15.** DSC analysis of star-shaped PHBs with MSSP with different arm lengths.

**Table 5.** Thermal properties of PHBs with glycerin with different arm lengths.<sup>a, b</sup>

Entry	[I]/[Zn]/[BBL]	$T_{max}$	$T_g$
Table 1, entry 2	3:1:300	-	5.3
Table 1, entry 3	3:1:600	300	8.0
Table 1, entry 4	3:1:1200	302	-2.6
Table 1, entry 5	3:10:600	298	4.9
Table 1, entry 6	3:20:600	-	-6.4

<sup>a</sup>Temperatures in °C. <sup>b</sup> $T_g$  values were determined from the second heating cycle in DSC.

**Table 6.** Thermal properties of PHBs with PE with different arm lengths.<sup>a, b</sup>

Entry	[I]/[Zn]/[BBL]	$T_{max}$	$T_g$
Table 2, entry 2	4:1:100	-	5.6
Table 2, entry 3	4:1:400	299	8.3
Table 2, entry 4	4:1:800	300	7.6
Table 2, entry 5	4:10:800	298	5.4

<sup>a</sup>Temperatures in °C. <sup>b</sup> $T_g$  values were determined from the second heating cycle in DSC.

**Table 7.** Thermal properties of PHBs with MSSP with different arm lengths.<sup>a, b</sup>

Entry	[I]/[Zn]/[BBL]	$T_{max}$	$T_g$
Table 3, entry 2	12:1:1200	-	6
Table 3, entry 3	12:1:2400	299	1.4
Table 3, entry 4	12:1:4800	302	2.5

<sup>a</sup>Temperatures in °C. <sup>b</sup> $T_g$  values were determined from the second heating cycle in DSC.

## 2.5 Thermogravimetric Analysis

Thermal stability of the star-shaped PHBs was analyzed by TGA carried out from 30 to 600 °C. Figure 16 shows a comparison of the thermal decomposition temperature of the synthesized PHBs with different arm numbers. The TGA data (in Table 4) and thermograms indicated that the onset ( $T_{-5\%}$ ) and the maximum decomposition ( $T_{max}$ ) of the star-shaped PHBs were lower than those of linear and cyclic PHBs. This reduced thermal stability could be related to the increase of thermally unstable hydroxyl groups.<sup>32</sup> The decomposition curve showed a single stage, and the PHBs with MSSP as a central core exhibited the fastest thermal decomposition. Remarkably, the PHB with PE showed a slightly higher  $T_{-5\%}$  value due to the decreased crystallinity of the obtained polymer. Comparatively, the thermal stability of the obtained PHBs decreased in the order PHB-glycerin>PHB-PE>PHB-MSSP, although they have the same arm lengths.

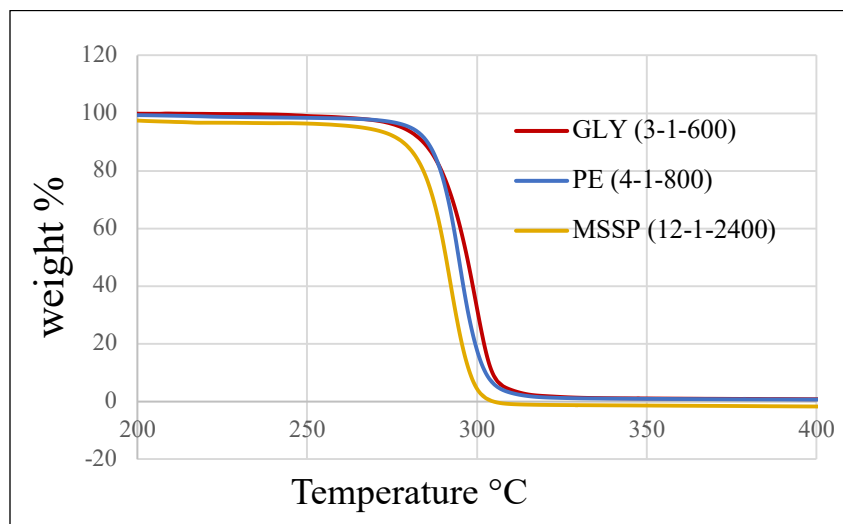


**Figure 16.** TGA analysis of star-shaped PHBs.

## Conclusions

In summary, a series of biodegradable and well-defined star-shaped and highly branched PHBs with different arm numbers and arm lengths were successfully synthesized using Zn catalyzed ROP of BBL in the presence of hydroxyl-terminated initiators. The efficient initiation by the three-, four-, and multi-armed cores was confirmed by the NMR analysis. The thermal properties of the obtained star-shaped PHBs depended upon their arm numbers as well as their arm lengths, showing that the thermal properties such as  $T_g$  and  $T_{max}$  could be modified by changing the arm numbers and arm lengths. The investigation of thermal stability could be effectively enhanced by the incorporation of higher functional alcohols. Future research will focus on expanding this methodology to include the incorporation of other monomers.

## REFERENCES

1. Philip, S.; Keshavarz, T.; Roy, I. Polyhydroxyalkanoates: Biodegradable Polymers with a Range of Applications. *J. Chem. Technol. Biotechnol.* **2007**, *82*, 233–247.
2. Gumel, A. M.; Annuar, M. S. M.; Chisti, Y. Recent Advances in the Production, Recovery and Applications of Polyhydroxyalkanoates. *J. Polym. Environ.* **2013**, *21*, 580–605.
3. Prasteen, P.; Thushyanthy, Y.; Mikunthan, T.; Prabhakaran, M. Bio-Plastics - an Alternative to Petroleum Based Plastics. *Int. J. Res. Stud. Agricultural Sci.* **2018**, *4*, 1–7.
4. Dunn, E.W.; Coates, G.W. Carbonylative Polymerization of Propylene Oxide: A Multicatalytic Approach to the Synthesis of Poly(3-Hydroxybutyrate). *J. Am. Chem. Soc.* **2010**, *132*, 11412–11413.
5. Xu, Y. C.; Ren, W. M.; Zhou, H.; Gu, G. G.; Lu, X. B. Functionalized Polyesters with Tunable Degradability Prepared by Controlled Ring-Opening (Co)polymerization of Lactones. *Macromolecules* **2017**, *50*, 3131–3142.
6. Grobelny, Z.; Golba, S.; Jurek-Suliga, J. Ring-opening polymerization of  $\beta$ -butyrolactone in the presence of alkali metal salts: investigation of initiation course and determination of polymers structure by MALDI-TOF mass spectrometry. *Polym. Bull.* **2018**, 1–16.
7. Ebrahimi, T.; Aluthge, D. C.; Hatzikiriakos, S.G.; Mehrkhodavandi, P. Highly Active Chiral Zinc Catalysts for Immortal Polymerization of  $\beta$ -Butyrolactone from Melt Processable Syndio-Rich Poly(hydroxybutyrate). *Macromolecules* **2016**, *49*, 8812–8824.
8. Bai, J.; Xiao, X.; Zhang, Y.; Chao, J.; Chen, X.  $\beta$ -Pyridylenolate Zinc Catalysts for the Ring-Opening Homo- and Copolymerization of  $\epsilon$ -Caprolactone and Lactides. *Dalton Trans.* **2017**, *46*, 9846–9858.

9. Deng, Y.; Liu, S. J.; Zhao, B. M.; Wang, P.; Fan, Q. L.; Huang, W.; Wang, L. H. Synthesis and Characterization of one Star-Shaped Polymer with Charged Iridium Complex as Luminescent Core. *J. Luminescence* **2011**, *131*, 2166–2173.
10. Ren, J. M.; McKenzie, T. G.; Fu, Q.; Wong, E. H. H.; Xu, J.; An, Z.; Shanmugam, S.; Davis, T. P.; Boyer, C.; Qiao, G. G. Star Polymers. *Chem. Rev.* **2016**, *116*, 6743–6836.
11. Michalski, A.; Brzezinski, M.; Lapienis, G.; Biela, T. Star-Shaped and Branched Polylactides: Synthesis, Characterization, and Properties. *Prog. Polym. Sci.* **2019**, *89*, 159–212.
12. Gadwal, I.; Wadgaonkar, P. P.; Ichake, A. B.; Mane S. R. A New Approach for the Synthesis of Miktoarm Star Polymers Through a Combination of Thiol–Epoxy “Click” Chemistry and ATRP/Ring-Opening Polymerization Techniques. *J. Polym. Sci., Part A: Polym. Chem.* **2019**, *57*, 146–156.
13. Cheng, J.; Ding, J. X.; Wang, Y. C.; Wang, J. Synthesis and Characterization of Star-Shaped Block Copolymer of Poly( $\epsilon$ -Caprolactone) and Poly(Ethyl Ethylene Phosphate) As Drug Carrier. *Polymer* **2008**, *49*, 4784–4790.
14. Pahl, P.; Schwarzenböck, C.; Herz, F. A. D.; Soller, B. S.; Jandl, C.; Riege, B. Core-First Synthesis of Three-Armed Star-Shaped Polymers by Rare Earth Metal-Mediated Group Transfer Polymerization. *Macromolecules* **2017**, *50*, 6569–6576.
15. Teng, L.; Xu, X.; Nie, W.; Zhou, Y.; Song, L.; Chen, P. Synthesis and Degradability of a Star-Shaped Polylactide Based on L-Lactide and Xylitol. *J. Polym. Res.* **2015**, *22*, 83–45.
16. Yu, I.; Ebrahimi, T.; Hatzikiriakos, S. G.; Mehrkhodavandi, P. Star-Shaped PHB–PLA block copolymers: immortal polymerization with dinuclear indium catalysts. *Dalton Trans.* **2015**, *44*, 14248–14254.



17. Lele, B.S.; Leroux, J.C. Synthesis of Novel Amphiphilic Star-Shaped Poly(1-caprolactone)-Block- Poly(N-(2-hydroxypropyl)methacrylamide) by Combination of Ring-Opening and Chain Transfer Polymerization. *Polymer* **2002**, *43*, 5595–5606.
18. Dirlam, P. T.; Goldfeld, D. J.; Dykes, D. C.; Hillmyer, M. A. Polylactide Foams with Tunable Mechanical Properties and Wettability using a Star Polymer Architecture and a Mixture of Surfactants. *ACS Sustainable Chem. Eng.* **2019**, *7*, 1698–1706.
19. Abbina, S.; Du, G. Zinc-catalyzed Highly Isolelective Ring Opening Polymerization of *rac*-Lactide. *ACS Macro. Lett.* **2014**, *3*, 689–692.
20. Abbina, S.; Chidara, V. K.; Bian, S.; Ugrinov, A.; Du, G. Synthesis of Chiral C<sub>2</sub>-symmetric Bimetallic Zinc Complexes of Amido-Oxazolinates and Their Application in Copolymerization of CO<sub>2</sub> and Cyclohexene Oxide. *ChemistrySelect* **2016**, *1*, 3175–3183.
21. Abbina, S.; Du, G. Chiral Amido-Oxazolate Zinc Complexes for Asymmetric Alternating Copolymerization of CO<sub>2</sub> and Cyclo- hexene Oxide. *Organometallics* **2012**, *31*, 7394–7403.
22. Abbina, S.; Chidara, V. K.; Du, G. Ring Opening Copolymerization of Styrene Oxide and Cyclic Anhydrides Using Highly Effective Zinc Amido-Oxazolate Catalysts. *ChemCatChem* **2017**, *9*, 1343–1348.
23. Shaik, M.; Peterson, J.; Du, G. Cyclic and Linear Polyhydroxylbutyrates from Ring-Opening Polymerization of  $\beta$ -Butyrolactone with Amido-Oxazolate Zinc Catalysts. *Macromolecules* **2019**, *52*, 157–166.

24. Chidara, V. K.; Stadem, S.; Webster, D. C.; Du, G. Survey of Several Catalytic Systems for the Epoxidation of a Biobased Ester Sucrose Soyate. *Catal. Commun.* **2018**, *111*, 31–35.
25. Binda, P. I.; Abbina, S.; Du, G. Modular Synthesis of Chiral  $\beta$ -Diketiminato-Type Ligands Containing 2-Oxazoline Moiety via Palladium-Catalyzed Amination. *Synthesis* **2011**, 2609–2618.
26. Nelson, T. J.; Masaki, B.; Morseth, Z.; Webster, D. C. Highly Functional Biobased Polyols and Their Use in Melamine–Formaldehyde Coatings. *J. Coat. Technol. Res.* **2013**, *10*, 757–767.
27. Wang, R.; Schuman, T. P. Vegetable Oil-Derived Epoxy Monomers and Polymer Blends: A Comparative Study with Review. *eXPRESS Polym. Lett.* **2013**, *7*, 272–292.
28. Salih, A. M.; Ahmad, M. B.; Ibrahim, N. A.; Dahlan, K. Z. H. M.; Tajau, R.; Mahmood, M. H.; Yunus, W. M. Z. W. Synthesis of Radiation Curable Palm Oil–Based Epoxy Acrylate: NMR and FTIR Spectroscopic Investigations. *Molecules* **2015**, *20*, 14191–14211.
29. Fazeli, N.; Mohammadi, N.; Taromi, F. A. A Relationship Between Hydrodynamic and Static Properties of Star-Shaped Polymers. *Polym. Testing* **2004**, *23*, 431–435.
30. Zhang, W.; Zheng, S. Synthesis and Characterization of Dendritic Star Poly(L-Lactide)s. *Polym. Bull.* **2007**, *58*, 767–775.
31. Guo, Z.; Chen, X.; Xin, J.; Wu, D.; Li, J.; Xu, C. Effect of Molecular Weight and Arm Number on the Growth and pH-Dependent Morphology of Star Poly[2-(dimethylamino)ethyl methacrylate]/Poly(styrenesulfonate) Multilayer Films. *Macromolecules* **2010**, *43*, 9087–9093.

32. Xie, W.; Jiang, N.; Gan Z. Effects of Multi-Arm Structure on Crystallization and Biodegradation of Star-Shaped Poly( $\epsilon$ -caprolactone). *Macromol. Biosci.* **2008**, *8*, 775–784.
33. He, J.; Liu, W.; Huang, Y. X. Simultaneous Determination of Glass Transition Temperatures of Several Polymers. *PLoS ONE* **2016**, *11*, 1–12.